# Journal Pre-proof
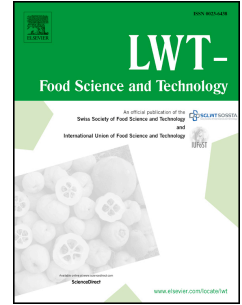
α-Dicarbonyl compounds trapping ability and antiglycative effect of high-molecular-weight brewer's spent grain melanoidins

Slim Blidi, Antonio Dario Troise, Moira Ledbetter, Sarah Cottin, Keith Sturrock, Sabrina De Pascale, Andrea Scaloni, Alberto Fiore

Please cite this article as: Blidi, S., Troise, A.D., Ledbetter, M., Cottin, S., Sturrock, K., De Pascale, S., Scaloni, A., Fiore, A., α-Dicarbonyl compounds trapping ability and antiglycative effect of high-molecular-weight brewer's spent grain melanoidins, *LWT - Food Science and Technology* (2023), doi: https://doi.org/10.1016/j.lwt.2023.114679.

This is a PDF file of an article that has undergone enhancements after acceptance, such as the addition of a cover page and metadata, and formatting for readability, but it is not yet the definitive version of record. This version will undergo additional copyediting, typesetting and review before it is published in its final form, but we are providing this version to give early visibility of the article. Please note that, during the production process, errors may be discovered which could affect the content, and all legal disclaimers that apply to the journal pertain.

**CRediT authorship contribution statement**

**Slim Blidi:** Conceptualization, Methodology, Investigation, Data curation, Formal analysis, Validation, Writing - original draft, Visualization.

**Antonio Dario Troise:** Investigation, Formal analysis, Writing - original draft, Writing – review & editing, Visualization, Resources.

**Moira Ledbetter:** Investigation, Writing – review & editing

**Sarah Cottin:** Writing - review & editing, Supervision

**Keith Sturrock:** Conceptualization, Supervision, Funding acquisition, Writing – review & editing

**Sabrina De Pascale**: Investigation, Formal analysis, Data curation, Resources

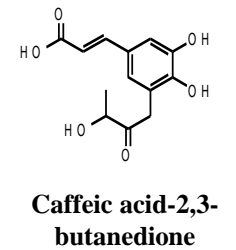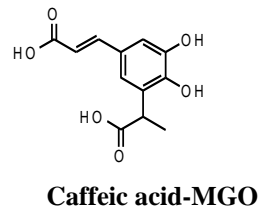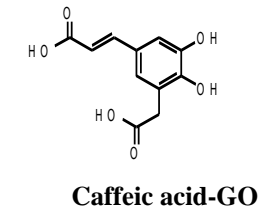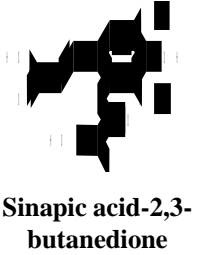**Andrea Scaloni**: Resources, Writing - review & editing, Project administration.

**Alberto Fiore**: Conceptualization, Supervision, Funding acquisition, Writing – review & editing, Project administration.
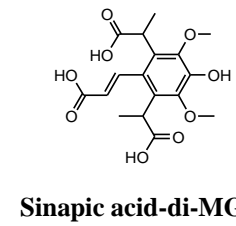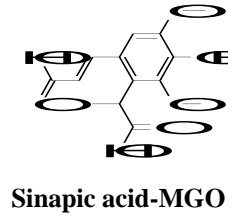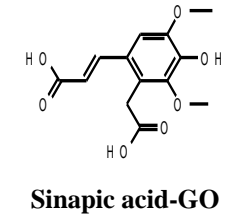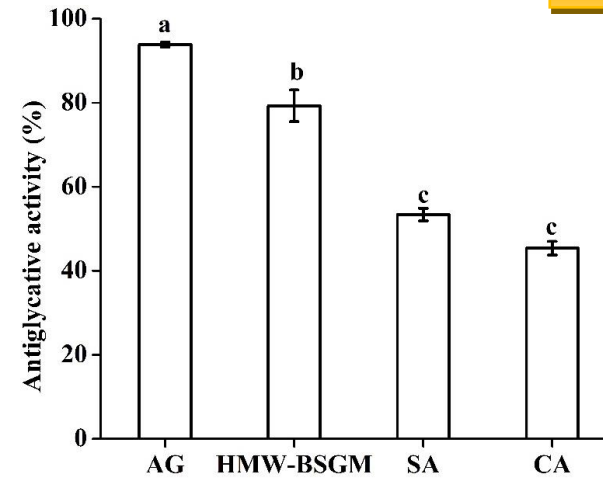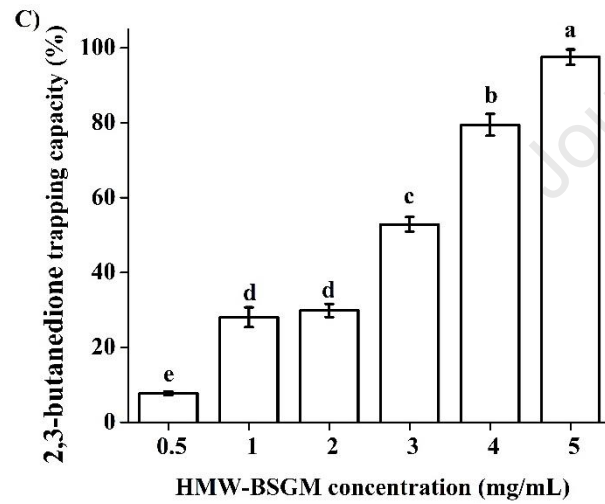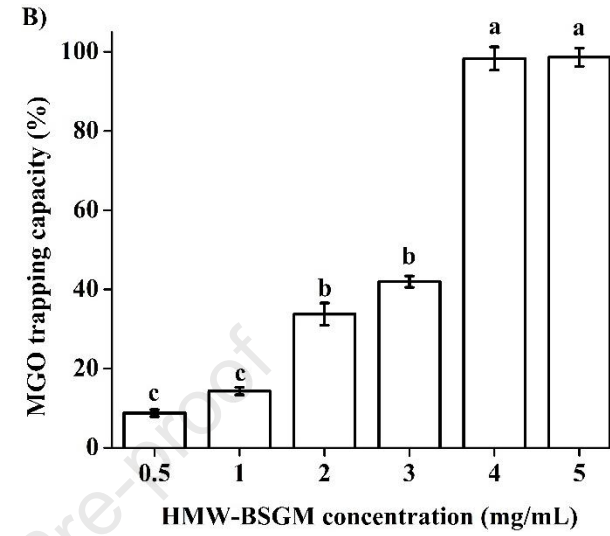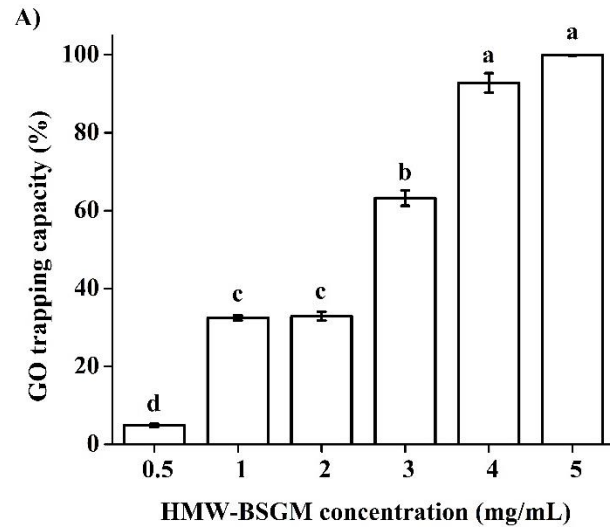
1 **α-Dicarbonyl compounds trapping ability and antiglycative effect of high-molecular-**

2 **weight brewer's spent grain melanoidins**

3 Slim Blidi[a], Antonio Dario Troise[b], Moira Ledbetter[a], Sarah Cottin[a], Keith Sturrock[c], Sabrina

4 De Pascale[b], Andrea Scaloni[b], Alberto Fiore[a*]

5

6 [a] School of Applied Sciences, Division of Engineering and Food Science, University of

7 Abertay, Bell Street, DD1 1HG, Dundee, Scotland, United Kingdom.

8 [b] Proteomics, Metabolomics & Mass Spectrometry Laboratory, Institute for the Animal

9 Production System in the Mediterranean Environment, National Research Council, 80055

10 Portici, Italy.

11 [c] School of Applied Sciences, Division of Psychology and Forensic Science, University of

12 Abertay, Bell Street, DD1 1HG, Dundee, Scotland, United Kingdom.

13 *Corresponding author: Alberto Fiore

14 email address: a.fiore@abertay.ac.uk

15 Tel: +44 1382 30 8043

16

17    **Highlights:**

18

19    A novel use of brewer's spent gain is discussed.

20    The polyphenolic profile of brewer's spent grain melanoidins is established.

21    Brewer's spent grain melanoidins trapped α-dicarbonyls in a simplified model system.

22    Brewer's spent grain melanoidins inhibited the formation of free fluorescent AGEs.

23    The putative adduct of sinapic acid-di-MGO is reported for the first time.

24  **Abstract**

25  Polyphenols participate in the Maillard reaction pathways scavenging α-dicarbonyl

26  compounds (DCs) and contributing to the mitigation of carbonyl burden through dietary

27  exposure/routes. The current study demonstrated the effectiveness of high-molecular-weight

28  brewer's spent grain melanoidins (HMW-BSGM) in reacting with DCs in an *in vitro* model

29  system. HMW-BSGM (4 mg/mL) quenched more than 95% of glyoxal and methylglyoxal,

30  and more than 80% of 2,3-butanedione after a 7-day incubation at 37 °C. Among tested

31  polyphenols, sinapic acid showed the highest trapping capacity with inhibition rates of 33.1,

32  49.1 and 49.3% for glyoxal, methylglyoxal and 2,3-butanedione because of

33  hydroxyalkylation as revealed by liquid chromatography high-resolution tandem mass

34  spectrometry experiments. The formation of free fluorescent AGEs was substantially

35  hindered (79.3%) by HMW-BSGM (4 mg/mL). These findings corroborate the hypothesis

36  that the local accumulation of polyphenols in melanoidins skeleton can hinder undesired

37  effects and potentially harmful reactions involving α-dicarbonyl compounds.

38

42 **Abbreviations**

43 2,3-MQX: 2,3-dimethylquinoxaline; 2-MQX: 2 -methylquinoxaline; 4-HBA: 4-

44 hydroxybenzoic acid; ABTS: 2,2′-azino-bis (3-ethylbenzothiazoline-6-sulfonic acid); AG:

45 aminoguanidine; AGEs: advanced glycation end-products; BSA: bovine serum albumin;

46 BSG: brewer's spent grain; DC: α-dicarbonyl compound; DNA: deoxyribonucleic acid; dw:

47 dry weight; EDTA: ethylenediaminetetracetic acid; ESI: electrospray ionization; FC: Folin-

48 Ciocalteu; FTMS: Fourier transform mass spectrometry; GAE: gallic acid equivalents; GI:

49 gastrointestinal; GLC: glucose; GO: glyoxal; HBAs: hydroxybenzoic acids; HCAs:

50 hydroxycinnamic acids; HMW-BSGM: high-molecular-weight brewer's spent grain

51 melanoidins; HPLC: high-performance liquid chromatography; HMW: high-molecular-

52 weight; HMWM: high-molecular-weight melanoidins; LC-HRMS/MS: liquid

53 chromatography coupled with high-resolution tandem mass spectrometry; LC-MS: liquid

54 chromatography coupled with mass spectrometry; LOD: limit of detection; LOQ: limit of

55 quantification; MGO: methylglyoxal; MRM: multiple reaction monitoring; OPD: o-

56 phenylenediamine; PM: pyridoxamine; PVDF: polyvinylidene fluoride; QX: 1-quinoxaline;

57 RSM: response surface methodology; TEAC: trolox equivalent antioxidant capacity; Trolox:

58 hydroxy-2,5,7,8-tetramethylchroman-2-carboxylic acid.

## 1. Introduction

59

60 Carbohydrate oxidation and the Maillard reaction lead to the formation of α-dicarbonyl

61 compounds (DCs). Among the most comprehensively studied DCs, glyoxal (GO),

62 methylglyoxal (MGO) and 2,3-butanedione are the prevalent precursors of advanced

63 glycation end-products (AGEs) (Lan et al., 2020).

64 Equally generated *in vivo*, DCs are known for their reactivity with amino acids such as lysine

65 and arginine (Hellwig et al., 2019) or , as recently reported, with tryptophan (Herraiz et al.,

66 2022) leading to the formation of a wide range of potentially harmful AGEs and β-carbolines.

67 DCs might contribute to the occurrence of multifactorial diseases including peripheral

68 neuropathy, kidney disease and obesity (Gaens et al., 2013; Sato et al., 2006), and their

69 excessive formation was established in diabetes (Brings et al., 2017). Moreover, DCs are

70 significant to the *in vivo* development of AGEs (Delgado-Andrade & Fogliano, 2018;

71 Rabbani & Thornalley, 2012) and may be involved in the carbonylation of lipids, proteins, or

72 DNA, altering normal physiological functions (Ahmad et al., 2014). High intake of processed

73 foods and dietary AGEs has been linked to both an increase in microvascular diseases as

74 chronic kidney disease and diabetes (Snelson et al., 2021). However, a direct link between

75 dietary AGEs and health outcomes is still a rationale to be fully proven. Indeed , besides the

76 multifactorial molecular aspects of the diet, some dietary AGEs, such as those buried within

77 inaccessible protein structures, are poorly digested reducing absorption by the gastrointestinal

78 (GI) tract, while low molecular dietary AGEs are eliminated through renal function (Sergi et

79 al., 2021).

80 DC trapping was demonstrated to be an effective approach to limit the extent of subsequent

81 downstream reactions resulting in unwanted traits in foods, and to hinder further damages *in*

82 *vivo* (Zhang et al., 2020). Besides synthetic compounds, natural food products and their

83    extracts, including aqueous isolates of peach, pomegranate and apricot seeds (Mesías et al.,

84    2013), guava leaf extracts (Wu et al., 2009), cinnamon bark (proanthocyanidins) (Peng et al.,

85    2008), stilbene glucoside from *Polygonum multiflorum* (Thunb.) (Lv et al., 2010),

86    blackcurrant anthocyanins (Chen et al., 2014), tea catechins, ginger shogaols (Huang et al.,

87    2017) and secoiridoids derivatives from olive leaf and oil (Troise et al., 2014), inhibit the

88    generation of DCs and contribute to their elimination.

89    Correlation of dietary intake and the *in vivo* concentration of DCs is yet to be established

90    when considering the complexity of dietary patterns. Recent studies suggested an association

91    between a DC-rich diet and endogenous MGO levels (Maasen et al., 2022), however,

92    confounding factors including dietary concentrations of lipids & proteins (Baynes & Thorpe,

93    2000; Davies, 2016) should be considered.

94    Because of their ubiquitous presence in foods, restricting the intake of DCs or trapping them

95    within the digestive system are interesting approaches that can limit the endogenous DC

96    concentration (Delgado-Andrade & Fogliano, 2018). Indeed, ingestion of pure dietary

97    flavonoids considerably contributed to a decline in the endogenous DCs concentrations (Van

98    den Eynde et al., 2018).

99    High-molecular-weight melanoidins (HMWM) are brown polymers formed during food

100    processing with a specific molecular structure depending on the food composition (Zhang et

101    al., 2019). Typical daily dietary intake for melanoidins is estimated to be 10.0 g (Fogliano &

102    Morales, 2011). Several studies demonstrated their antioxidant, antimicrobial, and prebiotic

103    capacities (Mesías & Delgado-Andrade, 2017; Palma-Duran et al., 2016). In general,

104    melanoidins perform as bioactive dietary fibre within the GI tract by enhancing the release of

105    reducing capacity in the presence of reductones and condensed polyphenols (Morales et al.,

106    2012). Polyphenols are integrated into melanoidin structures in coffee, cocoa, fruits, and

107    nuts. For example, coffee melanoidins contain fragments of chlorogenic acids (Coelho et al.,

108    2014), and epicatechins have been found in cocoa melanoidins (Oracz et al., 2019).

109    The array of reactive moieties and polyphenols present on melanoidin skeleton can work as a

110    trapping agent for dicarbonyls. In this context, Zhang et al. demonstrated greater than 40%

111    DC trapping after 2 h from HMW coffee melanoidins, under physiological conditions (Zhang

112    et al., 2019).

113    Brewer's spent grain (BSG) represents a functional matrix rich in both polyphenols and

114    carbohydrates. Despite the fact that BSG contains a considerable load of  polyphenols, it is

115    underutilized and is primarily used in animal feed (Kasperovich et al., 2009). More recently,

116    BSG was utilised as a substrate for the production of enzymes, lactic acid, bioethanol, and

117    xylitol (Nigam, 2017). However, the trapping capacity of BSG toward DCs is yet to be

118    investigated and could have the potential benefit of adding value to this by-product.

119    This study aimed to assess the DCs trapping capacity of HMWM from roasted BSG (HMW-

120    BSGM) in a model *in vitro* system and to identify mechanisms crucial to the trapping

121    activity, thus exploring the possibility to valorise BSG as a bioactive source of antiglycative

122    compounds.

123    **2.  Materials and methods**

124    **2.1.  Chemicals and reagents**

125    GO aqueous solution (40%), MGO aqueous solution (40%), 2,3-butanedione, pyridoxamine

126    (PM) dihydrochloride, o-phenylenediamine (OPD), ethylenediaminetetracetic acid (EDTA),

127    caffeic acid, (+)-catechin, ferulic acid, sinapic acid, 4-hydroyxbenzoic acid, syringic acid,

128    vanillic acid, vanillin, p-coumaric acid, benzoic acid, protocatechuic acid, gallic acid, 2,2′-

129    azino-bis (3-ethylbenzothiazoline-6-sulfonic acid) (ABTS) diammonium salt,

130    aminoguanidine (AG) hydrochloride, bovine serum albumin (BSA), glucose (GLC),

131    penicillin-G sodium salt, sodium azide (NaN$_3$) and formic acid were purchased from Sigma-

132    Aldrich (St. Louis, MO). Hydrochloric acid (HCl, 37%), sodium hydroxide (NaOH),

133    methanol HPLC grade, acetonitrile HPLC and LC-MS grades, 6-hydroxy-2,5,7,8-

134    tetramethylchroman-2-carboxylic acid (Trolox), potassium persulfate, and NaCl were

135    obtained from Thermo Fisher Scientific (Waltham, MA). Sodium dihydrogen phosphate

136    dihydrate (NaH$_2$PO$_4$·2H$_2$O), di-sodium hydrogen phosphate dihydrate (Na$_2$HPO$_4$·2H$_2$O) and

137    Folin-Ciocalteu′s (FC) phenol reagent were purchased from Merck (Darmstadt, Germany).

138    **2.2.   Brewer's spent grain source and high-molecular-weight brewer's spent grain**

139        **melanoidins (HMW-BSGM) preparation**

140    BSG originating from the *Concerto* barley variety were provided by a local distillery in Fife,

141    Scotland. The fresh BSG was dried at 60 °C overnight using a convection oven (Memmert,

142    Schwabach, Germany), and then stored in an air-tight container before further use. HMW-

143    BSGM were obtained according to the method of  Summa et al. (2006) with some

144    modifications. BSG were roasted in a convection oven (Memmert, Schwabach, Germany)

145    according to nine different roasting regimes increasing in time (30, 60 and 90 min) and

146    temperature (160, 185 and 210 °C). Roasted BSG was ground using a ring sieve of 0.5 mm in

147    diameter fitted to an electric mill (ZM 200, Retsch, Haan, Germany). Roasted BSG powder

148    (100 g) was extracted in water (1.2 L) for 20 minutes at 80 °C, with stirring. The supernatant

149    was filtered under vacuum (Whatman 595, Billerica, MA). The filtrate was dialyzed (MW

150    cut-off 14 kDa, D9402, Sigma-Aldrich, St. Louis, MO) at 4 °C, until conductivity was ≤ 2

151    µS/cm, as measured by a conductivity meter (DiST 3, Hanna Instruments, Woonsocket, RI)

152    (water renewed at rate of 1 L per cycle) allowing the removal of any potential remaining free

153    sugars and amino acids as well as polypeptide chains of up to 140 amino acids. Retentate was

154 stored at -20 °C prior to and post freeze drying. The yield of melanoidin content was

155 determined by weighing the freeze-dried product and was ranging between 1.11 and 2.43 g of

156 melanoidin extract/100 g of roasted BSG, depending on the roasting intensity.

157 **2.3. Response surface methodology design**

158 The roasting procedure of BSG was optimized utilizing a response surface methodology

159 (RSM) experimental design. A face-centred two factor composite design consisting of 10

160 randomised runs, with two centre-point replicates was used. Roasting temperature (160, 185

161 and 210 °C, $X_1$) and roasting duration (30, 60 and 90 min, $X_2$) were the independent

162 variables. The total phenolic content  and the antioxidant activity of HMW-BSGM were the

163 two dependent variables. A second polynomial response surface was used to fit the

164 experimental data following Equation 1 (Iglesias-Carres et al., 2019):

$$Y = \beta_0 + \sum_{i=1}^2 \beta_i X_i + \sum_{i=1}^2 \beta_{ii} X_{ii}^2 + \sum_{i=1} \sum_{j=i+1} \beta_{ij} X_{ii} X_{ji} \quad (1)$$

166 Where Y is the dependent variable, $\beta_0$ is the constant coefficient, and $\beta_i$, $\beta_{ii}$, and $\beta_{ij}$ are the

167 linear, quadratic, and interaction regression coefficients, respectively. $X_i$, $X_{ii}$, and $X_{ji}$

168 represent the independent variables.

169 **2.4. Analysis of response variables of response surface methodology design**

170 Analysis of response surface variables required the determination of the following

171 experimental endpoints (antioxidant activity and total phenolic content) was performed as

172 described below.

### 2.4.1. Determination of the antioxidant activity of HMW-BSGM

The antioxidant activity of HMW-BSGM from the three different roasting regimes was estimated following a previously described method (Re et al., 1999) with minor modifications. Prior to antioxidant activity determination, acid hydrolysis was performed as per section 2.5.1.a., accounting for total antioxidant activity. ABTS radical cations (ABTS•+) were produced to get an absorbance between 0.70 and 0.75 at 734 nm. Melanoidin hydrolysate (10 mg/mL) or Trolox standard (100 µL) added to 1.0 mL of diluted ABTS•+ solution, an absorbance reading at 734 nm was taken after 2.5 minutes using a UV-Vis spectrophotometer (Thermo Scientific Genesys 10S, Waltham, MA). External calibration with a linear range 10-250 µmol/L was used to express results as Trolox equivalent antioxidant capacity (TEAC) in mg per 100 g of dry weight (mg TEAC/100 g dw).

### 2.4.2. Determination of total phenolic content of HMW-BSGM

The total phenolic content in the extracts was analysed by the FC method (Singleton et al., 1999) with minor modifications. Total phenolic content determination was preceded by the same acidic hydrolysis procedure described in section 2.5.1.a. Analysis was scaled to a sample aliquot of 125 µL of each HMW-BSGM hydrolysate (10 mg/mL). The initial incubation period was 6 mins. Following dilution, the second incubation period was for 90 min, in the dark, at room temperature, absorbance was measured at 760 nm (Thermo Scientific Genesys 10S UV-Vis Spectrophotometer, Waltham, MA). An external calibration curve was constructed using aqueous gallic acid standard solutions ranging in concentrations from 10 to 200 µg/ml. The total phenolic content of the samples was expressed as gallic acid equivalents (GAE) in mg per 100 g of dry weight (mg GAE/100 g dw).

195 **2.5. Characterisation of phenolic compounds present in HMW-BSGM**

196 **2.5.1. Release of bound phenolic compounds from HMW-BSGM**

197 **a. Acidic hydrolysis**

198 Prior to analysis, acidic hydrolysis was performed to release bound polyphenols from HMW-

199 BSGM according to the method of Oracz et al. (2019) with the following modifications. 1.0

200 mL of HCl (10 M) was mixed with HMW-BSGM (2.5 mL, 40 mg/mL in 50% v/v aqueous

201 methanol). Following hydrolysis and neutralisation, the supernatant was evaporated under

202 vacuum using a rotary evaporator (Eppendorf Concentrator 5310, Hamburg, Germany) and

203 redissolved in 2.5 mL of 50% v/v aqueous methanol to a final concentration of 10 mg/mL. A

204 control sample was prepared as follows: 50 mg of non-treated HMW-BSGM was dissolved in

205 4.75 mL of water then centrifuged (4500$g$ for 8 min at 4 °C). The supernatant was then

206 filtered using a 0.22 μm PVDF filter.

207 **b. Alkaline hydrolysis**

208 Alkaline hydrolysis of HMW-BSGM was carried out in order to release covalently-bound

209 polyphenols following the method of Coelho et al. (2014) with  modifications. Initial

210 melanoidin concentration of 20 mg/mL in NaOH and incubation time increased to 90

211 minutes.

212 **2.5.2. Analysis of predominant phenolic compounds in HMW-BSGM**

213 The identification and quantification of predominant polyphenols in acid and alkali-

214 hydrolysed HMW-BSGM was achieved by liquid chromatography tandem mass spectrometry

215 (LC-MS/MS) according to Schulz et al. (2015) with some modifications. The

216 chromatographic separation was performed on a Synergi Hydro-RP 80 Å column (150 mm ×

217    4.6 mm, 4 μm, Phenomenex, Torrance, CA). Mobile phase A was 0.1% v/v formic acid

218    aqueous solution, and mobile phase B was 0.1% v/v formic acid in acetonitrile. The gradient

219    of solvent B (minutes/%B) was as follows: (0/10), (2/10), (9/90), (14/90), (14.1/10), (17/10).

220    The flow rate was 0.3 mL/min, and the column oven was set at 40 °C. The TSQ triple

221    quadrupole mass spectrometer mass spectrometer (Thermo Fisher Scientific, Waltham, MA)

222    was equipped with an electrospray ionisation (ESI) source and was operated in negative

223    ionisation mode. The ion source conditions were: spray voltage 4.0 kV, capillary temperature

224    270 °C, nitrogen was used as a nebulizer gas. Sheath and auxiliary nitrogen gas were used at

225    a flow rate of 50 and 25 arbitrary units, respectively. Polyphenols were quantified using their

226    respective external calibration standard curves. Retention time, Multiple reaction monitoring

227    (MRM) transitions, collision energy, linear calibration range, limit of detection (LOD), and

228    limit of quantification (LOQ) of each phenolic compound are listed in Table S1. Data were

229    collected with Xcalibur version 3.0 (Thermo Fisher Scientific, Waltham, MA).

230    **2.6.  Monitoring of the α-dicarbonyl trapping capacity of phenolic acids and HMW-**

231         **BSGM, time-course study and evaluation of the physiological relevance**

232    Sample preparation was performed according to the method described by Zhang et al. (2019)

233    with minor modifications. MGO, GO, 2,3-butanedione, sinapic acid, caffeic acid, ferulic acid,

234    4-hydroxybenzoic acid, syringic acid, vanillic acid, p-coumaric acid, benzoic acid,

235    protocatechuic acid, gallic acid and PM (positive control) were individually dissolved in

236    phosphate buffer (0.1 mol/L, pH 7.4) reaching the same molarity (6.4 mmol/L). GO, MGO,

237    or 2,3-butanedione (100 μL) was combined with 100 μL of PM solution (positive control)/

238    phosphate buffer (blank)/phenolic standard or melanoidin solutions (5 – 50 mg/mL) and 800

239    μL of phosphate buffer. Mixtures were then incubated at 37 °C, for 168 h. The final

240    concentrations of HMW-BSGM in model systems ranged from 0.5 to 5 mg/mL, whereas that

241    of DCs and PM/phenolic standards was 0.64 mmol/L. Following the incubation period, 0.2%

242    OPD solution (200 µL) containing EDTA (9.6 mmol/L) was added to the samples to

243    derivatise GO, MGO and 2,3-butanedione into and 1-quinoxaline (QX), 2 -methylquinoxaline

244    (2-MQX) and 2,3-dimethylquinoxaline (2,3-MQX), respectively. Prior to high-performance

245    chromatography (HPLC) analysis, samples were filtered through a 0.22 m PVDF filter after

246    vortexing for 5 s and incubating at 37 °C in the dark for 2 hours.

247    The HPLC analysis of the samples was performed according to the method of Ledbetter et al.

248    (2021) with minor modifications. The HPLC system consisted of a Thermo Fisher Scientific

249    Ultimate 3000 Pump (Waltham, MA), coupled with a Dionex DDA-100 diode array detector,

250    and a Dionex autosampler ASI-100 (San Jose, CA), equipped with 5 µm Eclipse Plus C18

251    column (150 mm × 4.6 mm) (Agilent, Santa Clara, CA), thermostated at 40 °C, at a flow rate

252    of 0.4 mL/min; the injection volume was 5 µL. A binary solvent system gradient of water

253    containing 0.1% v/v formic acid (A) and acetonitrile containing 0.1% v/v formic acid (B) was

254    used as follows (minutes/%B): (0/2), (2/2), (8/20), (10/40), (13/95), (16/95). Chromatograms

255    were recorded at 313 nm. QX, 2-MQX and 2,3-MQX eluted at 12.48 and 13.86 and 14.51

256    min, respectively. Peaks were identified and quantified, by comparison of retention time of

257    external calibration standards in the range 0.1–40 µg/mL. LOD was 0.008, 0.010 and 0.025

258    µg/mL for QX, 2-MQX and 2,3-MQX, respectively, while LOQ was 0.024, 0.033 and

259    0.083µg/mL for QX, 2-MQX and 2,3-MQX, respectively.

260    Percentage decrease in each DC was calculated using equation 2:

261        Trapping capacity (%) = [(DC in blank − DC in sample)/ DC in blank] × 100    (2)

262    Simulating the upper intestinal phase conditions, the estimated dietary daily intake of MGO

263    (1.9 mg/person) (Hellwig et al., 2018) and that of total melanoidins (10 g/person per day)

264    (Fogliano & Morales, 2011) were reacted together to evaluate the physiological significance

265    of DCs scavenging ability of HMW-BSGM. Assuming a digestive volume of 2 L, volumes

266    were scaled down as follows. 100 µL of GO/MGO/2,3-butanedione (0.26 mmol/L) was

267    incubated with 100 µL of HMW-BSGM (50 mg/mL) and 800 µL of phosphate buffer (0.1 M,

268    pH 7.4) at 37 ° for 2, 4 and 24 h. Then, solutions were derivatised and analysed by HPLC as

269    previously described.

270    **2.7.    Adducts confirmation by liquid chromatography high-resolution tandem mass**

271    **        spectrometry (LC-HRMS/MS)**

272     Acidic melanoidins extract (4 mg/mL) and polyphenols identified following the analysis in

273    section 2.5.2 (at the concentration levels used in section 2.6), were individually incubated

274    with GO, MGO and 2,3-butanedione (0.46 mg/mL) at 37 °C, for 168 h. The melanoidin

275    sample was subjected to acidic hydrolysis post incubation as described in section 2.5.1.a. to

276    release the formed adducts from the melanoidins matrix. Sample analysis was conducted with

277    a Vanquish Core LC system coupled with a quadrupole Orbitrap high resolution mass

278    spectrometer (Exploris 120, Thermo Fisher Scientific, Waltham, MA). Aqueous supernatants

279    were freeze-dried, then resuspended in methanol/water 70:30 (v/v) and 1 µL was directly

280    injected. Polyphenol-DC adducts were separated at 35°C through a core-shell biphenyl

281    column (Kinetex biphenyl, 100 x 2.1, 2.6 µm, Phenomenex, Torrance, CA) with the

282    following gradient of solvent B (minutes/%B): (0/5), (1.5/5), (13/90), (15/90). Mobile phases

283    consisted of water containing 0.1% formic acid (A) and acetonitrile (B) and the flow rate was

284    0.25 mL/min.  For negative ion mode H-ESI interface parameters were as follows: spray

285    voltage -3.2 kV, ion transfer tube and vaporizer temperature were 300 and 290 °C,

286    respectively; sheath gas flow and auxiliary gas flow were 45 and 10 arbitrary units. Upon a

287    preliminary screening in full scan mode in the *m/z* range 80-600, polyphenol-DC adducts

288    were tentatively identified in product ion scan mode screening the precursor ions according to

289    an in-house mass list generated in Trace Finder environment (v. 5.1, Thermo Fisher

290    Scientific, Waltham, MA) (Table S2). For product ion scan, normalized collision energy was

291    set at 30%, Orbitrap resolution at 30000 (FWHM at $m/z$ 200) and the quadrupole resolution

292    was set at 1. Profile data were collected using Xcalibur 4.5 (Thermo Fisher Scientific,

293    Waltham, MA) and fragmentation spectra were recorded by using Free Style software (v. 1.8,

294    Thermo Fisher Scientific, Waltham, MA).

295    **2.8.    Assessment of the *in vitro* glycation of bovine serum albumin with glucose**

296    The BSA-GLC assay was conducted following the method of Navarro et al., (2018) with

297    modifications. In brief, AG (4 mg/mL, positive control), HMW-BSGM (28 mg/mL), sinapic

298    acid (0.98 mg/ mL) and caffeic acid (0.77 mg/mL) were separately dissolved in phosphate

299    buffer (0.1 mol/L, pH 7.4).  An aliquot of 100 µL of each solution or of phosphate buffer

300    (blank) was added to 200 µL of a 175 mg/mL GLC solution and 200 µL of a 35 mg/mL BSA

301    solution (containing 0.1 mg/mL of $NaN_3$, 1.3 mg/mL of EDTA and 0.05 mg/mL of penicillin-

302    G). Solutions including samples, positive control and blank were incubated for 21 days, at 37

303    ˚C. The reference (without incubation) was kept at −20 °C for the same duration. To account

304    for potential interferences arising from the inhibitors, the intrinsic fluorescence of the

305    prepared solutions was estimated by separately mixing 100 µL of AG, HMW-BSGM, sinapic

306    acid and caffeic acid with 600 µL of phosphate buffer (0.01 mol/L, pH 7.4) and incubating

307    the mixture for 21 days, at 37 ˚C. The fluorescence intensity of all solutions was measured

308    using a spectrofluorometer (RF -1501, Shimadzu, Kyoto, Japan). Glycation was determined

309    by measuring fluorescence of solutions using excitation and emission maxima of 360 and 420

310    nm, respectively. The intrinsic fluorescence of each solution was deducted from its

311    corresponding total fluorescence in the BSA-GLC system. The inhibition percentage of

312    AGEs formation in each sample was determined following equation 3:

313    Inhibition (%) = {1 − [(fluorescence of solution with inhibitor - intrinsic fluorescence of

314    sample with inhibitor)/(fluorescence of blank solution - intrinsic fluorescence blank

315    solution]} × 100  (3)

316    **2.9.    Statistical analysis**

317    Analysis of RSM design results was performed using JMP 16.2 software (SAS Institute,

318    Cary, NC). Significant differences ($p < 0.05$) in the DC trapping, the antiglycative capacities

319    of samples and in the content of individual phenolic compounds in HMW-BSGM were

320    analysed by Tukey's HSD test and the Student's $t$-test using the SPSS statistics (v. 26.0,

321    IBM, Armonk, NY). Error bars in all figures express the standard deviation (SD). All

322    experiments were performed in triplicate.

323    **3.   Results and discussion**

324    **3.1.   Surface response results**

325    Experimental values of antioxidant activity and total phenolic content of HMW-BSGM

326    (dependent variables) quantified by spectrophotometry and the setting of the face-centred

327    design of roasting time and temperature (independent variables) are reported in Table S3. It is

328    demonstrated that roasting regimes affected the individual responses for the dependent

329    variables.

330    A summary of the regression coefficients of the model (Equation 1) for antioxidant activity

331    and total phenolic content obtained by the multiple linear regression can be found in Table

332    S4. The linear effects of the independent variables, their interaction and the quadratic were all

333  significant ($p < 0.05$) for antioxidant activity and total phenolic content. RSM surface plots

334  illustrating the statistical significance of the roasting time and temperature on the antioxidant

335  activity (Figure S1A) and the total phenolic content (Figure S1B) of HMW-BSGM show that

336  the two responses were similarly influenced by the two independent variables. Temperature

337  had a positive linear effect on both dependant variables while duration and temperature

338  showed a negative quadratic effect on antioxidant activity and total phenolic content,

339  meaning that the levels of both variables increase when the temperature and/or duration

340  increases up to a maximum, after which they reach a plateau then decrease (Figure S1 and

341  Table S4). This trend is in disagreement with a previous study on maize kernels (Youn &

342  Chung, 2012), in which extracted polyphenols increased in yield with rising roasting

343  temperature and time up to 240 ℃ and 50 min, respectively. This can be explained by the fact

344  that the softening of the kernel texture and the decomposition of insoluble polymer kernel

345  require a higher roasting temperature (Kahyaoglu & Kaya, 2006; Deshpande & Aguilar,

346  1975) than BSG, which consisted only of the outer shell of barley. This can also be attributed

347  to the more extreme conditions when roasting time exceeded 60 min causing the oxidation of

348  polyphenols and the formation of a very intricate molecular network. As shown in Table S5,

349  model validation data at the highest desirability (0.813) demonstrated that the optimal

350  roasting conditions to be used for the following part of the study were a temperature of

351  185.46 ℃ and a duration of 60.31 min.

352  **3.2.  Characterisation of melanoidin-bound polyphenols**

353  Upon acidic and alkaline hydrolyses of HMW-BSGM, concentration values of polyphenols

354  were determined as shown in Table 1. Melanoidin-bound polyphenols consisted mainly of

355  phenolic acids and their relative distribution showed a higher proportion of hydroxycinnamic

356    acids (HCAs) than hydroxybenzoic acids (HBAs) ($p < 0.05$). This was previously reported in

357    studies on phenolic content in BSG (Szwajgier et al., 2010).

358    The most abundant HCA was ferulic acid in the HMW-BSGM following acidic or alkaline

359    hydrolysis treatments, followed by p-coumaric acid and caffeic acid. This is in agreement

360    with previous studies on acids content of BSG following alkali hydrolysis (Hernanz et al.,

361    2001; McCarthy et al., 2013; Robertson et al., 2010), microwave-assisted alkaline hydrolysis

362    (Athanasios et al., 2007) and enzymatic hydrolysis (Szwajgier et al., 2010).

363    Syringic acid was the most represented HBA, while 4- hydroxybenzoic, vanillic, and

364    protocatechuic acids were 65.7, 49.7 and 17.3% toward syringic acid, respectively; which is

365    in agreement with previous work on the polyphenols concentration of alkali-hydrolysed BSG

366    samples (Athanasios et al., 2007).

367    When assessing the effect of the hydrolysis method on the phenolic content of HMW-BSGM,

368    acidic treatment released significantly higher amounts of polyphenols than alkaline

369    hydrolysis ($p < 0.05$). Furthermore, the individual polyphenols contents of the acidic and

370    alkaline extracts of HMW-BSGM were significantly different ($p < 0.05$) (Table 1).

371    For the acidic extract of the analysed HMW-BSGM samples, syringic, 4-hydroxybenzoic,

372    protocatechuic, ferulic, p-coumaric, sinapic and caffeic acids as well as catechin were all

373    detected at higher concentration. Whilst for the alkaline extract, benzoic, vanillic, gallic acids

374    and vanillin were detected at higher concentration.

375    Overall, higher amounts of HCAs were released by acid-catalysed treatment than by alkaline-

376    catalysed hydrolysis. Previous studies described a similar trend, where alkaline treatment

377    resulted in incomplete release of bound polyphenols present in HMW melanoidins (Moreira

378    et al., 2017; Monente et al., 2015; Coelho et al., 2014). The higher temperature applied to the

379    acidic treatment, may be attributed to the observed results. Due to increased likelihood, the

380    covalent linkages between polyphenols and branched macromolecules break allowing the

381    release of more bound polyphenols. Another contributory factor is functional group reactivity

382    (amide, carboxylic or hydroxyl groups) of polyphenols implicated in intermolecular

383    interactions occurring during acidic and alkaline hydrolyses (Oracz et al., 2019).

384    **3.3.    Monitoring of the α-dicarbonyl trapping capacity of phenolic acids and HMW-**

385    **BSGM, time-course study and evaluation the physiological relevance**

386    DC trapping capacities of the phenolic acids identified in HMW-BSGM are reported in

387    Figure 1. Sinapic acid showed the highest trapping capacity among the tested phenolic

388    standards with inhibition rates of $49.1 \pm 2.7$, $33.1 \pm 3.2$ and $49.3 \pm 1.6\%$ for MGO, GO and

389    2,3-butanedione, respectively, after a 7-day incubation. Caffeic acid also quenched $19.0 \pm$

390    $0.7$, $26.1 \pm 1.3$ and $34.5 \pm 3.1\%$ of GO, MGO and 2,3-butanedione, respectively, under the

391    same incubation conditions. In the tested conditions, HBAs did not show any significant DC

392    trapping ability.

393    A concentration range of 0.5-5 mg/mL for HMW-BSGM for DC trapping, was studied. The

394    DCs trapping capacity of HMW-BSGM was dose dependent, all DCs were effectively

395    trapped by HMW-BSGM when the concentration of melanoidins exceeded 2 mg/mL (Figure

396    2). More than 95% of GO and MGO and more than 80% of 2,3-butanedione was scavenged

397    by HMW-BSGM at a concentration of 4 mg/mL, following a 7-day incubation. HPLC

398    chromatograms of each studied DC in the presence of sinapic acid, caffeic acid and HMW-

399    BSGM (4mg/mL) are shown in Figure S2.These results support previous findings from

400    Zhang et al. (2019), who did not detect any of the three DCs after an incubation period of 7

401    days with coffee and cocoa melanoidins (2.5 mg/mL).

402    Based on these results, a time-course study including HMW-BSGM (4 mg/mL), sinapic acid,

403    caffeic acid and PM (positive control, a common carbonyl scavenger) to better understand the

404    reaction between polyphenols standards/polyphenols in HMW-BSGM and DCs.

405    Data of HMW-BSGM, sinapic acid, caffeic acid and PM DCs trapping capacities over time

406    are reported in Figure 3. GO concentration was reduced by $20.3 \pm 2.3\%$ and $18.2 \pm 0.3\%$ by

407    sinapic and caffeic acids, respectively, within 96 h. HMW-BSGM was a faster scavenger,

408    trapping $32.4 \pm 0.2\%$ within the first 48 h.

409    A similar trend was observed respecting MGO and 2,3-butanedione. HMW-BSGM showed a

410    higher trapping capacity ($40.4 \pm 0.8\%$) than sinapic acid ($30.8 \pm 1.4\%$) and caffeic acid ($8.1 \pm$

411    $0.2\%$) within the first 72 h of incubation with MGO, while incubation with 2,3-butanedione

412    for 24 h led to decreases of $25.3 \pm 1.9$, $9.2 \pm 0.5$ and $5.4 \pm 0.7\%$ by HMW-BSGM, sinapic

413    and caffeic acid, respectively.

414    HMW-BSGM DCs trapping capacities increased continuously during incubation to reach

415    maxima of $92.6 \pm 0.5$, $98.2 \pm 1.0$ and $83.2 \pm 1.6\%$ towards GO, MGO and 2,3-butanedione,

416    respectively.

417    The amount of DCs scavenged by sinapic and caffeic acids increased slowly upon longer

418    incubation time, reaching significantly lower values than those of HMW-BSGM. In fact,

419    sinapic acid scavenged $31.6 \pm 2.4$, $47.8 \pm 1.5$ and $49.1 \pm 1.6\%$ of GO, MGO and 2,3-

420    butanedione, respectively, after 168 h, while caffeic acid inhibited $23.5 \pm 3.2$, $26.4 \pm 1.4$ and

421    $37.5 \pm 2.2\%$ of GO, MGO and 2,3-butanedione, respectively, under the same conditions.

422    PM demonstrated a distinct DCs trapping ability; it was an effective MGO scavenger, a

423    moderate 2,3-butanedione scavenger and a poor GO scavenger. The current outcome parallels

424    prior findings, in which the most effective DC in reacting with amino groups was MGO,

425    particularly with PM (known for its capability to form stable heterocyclic compounds)

426    (Meade et al., 2003; Voziyan et al., 2002).

427    The time course study findings agree with those reported by Zhang et al. (2019) that pointed

428    out that coffee melanoidins (2 mg/mL) trapped almost all three DCs within 168 h of

429    incubation. However, the concentration of melanoidins in the current study is double that

430    investigated by Zhang and co-workers due to a lower polyphenols concentration in HMW-

431    BSGM compared to coffee melanoidins (Moreira et al., 2012; Coelho et al., 2014).

432    DCs trapping ability by HMW-BSGM, assessed the melanoidin fraction at a physiological

433    significant concentration (10 g/day/person) (Fogliano & Morales, 2011), based on the

434    assumption that melanoidins would accumulate in a volume around 2 L within 24 h (Rogalla

435    et al., 2005), HMW-BSGM were assayed at a concentration of 5 mg/mL.

436    Results summarised in Figure 4 demonstrated that about 50% of GO and MGO, and 25% of

437    2,3-butanedione were quenched within 2 h by HMW-BSGM. DCs trapping capacities

438    increased within time to reach around 85% for the three DCs after 24 h. These results

439    revealed that HMW-BSGM should be efficient in inhibiting DCs in both the intestinal tract

440    (within 2 h) and in the colon (up to 24 h). The poor bioaccessibility and bioavailability of

441    melanoidins can modulate the gut microbial population, and fermentation by specific

442    microorganism populations can be another invaluable and yet underexplored triggering factor

443    to release polyphenols and enhance their trapping activity (Vitaglione et al., 2012). Therefore,

444    there is evidence that HMW-BSGM are potentially effective in mitigating carbonyl content *in*

445    *vivo,* along with their ability to scavenge transition metals and other oxidizing counterparts.

446 **3.4. Adduct confirmation by LC-HRMS/MS**

447 The formation of DCs-caffeic acid and DCs-sinapic acid adducts in the DCs-polyphenols and

448 DCs-HMW-BSGM mixtures upon incubation at 37 °C, for 168 h is summarized in Figures 5

449 and 6. All the compounds reported in Table S2 were separated in acetonitrile gradient and

450 their elution profiles were in line with the presence of a substituted aromatic rings interacting

451 with biphenyl stationary phase. Full scan acquisition in the *m/z* range 80-600 in negative ion

452 mode pinpointed chemical formulas and their respective *m/z* signals for each of the chemical

453 structure with a mass tolerance of 5 ppm, thus suggesting electrophilic aromatic substitution

454 reactions or hydroxyalkyation reactions with MGO, GO and 2,3-butanedione (Totlani &

455 Peterson, 2006). Figure 5 outlines the fragmentation spectra of sinapic acid and sinapic acid-

456 DCs adducts in targeted $MS^2$ product ion scan experiments. Figure 5A shows the typical

457 fragmentation pattern of sinapic acid with the formation of molecular ion [M-H]$^-$ at *m/z*

458 223.0613 (mass error 0.4 ppm) and the product ions at *m/z* 208.0381, 193.0143, indicating the

459 typical loss of $CO_2$ [M-44]$^-$ and 149.0243 in line with publicly available database (MassBank

460 consortium and its contributors, 2020) and with previous results obtained by LC-ESI-linear

461 ion trap Orbitrap (Quifer-Rada et al., 2015). Figure 5 from B to D shows the spectra of

462 sinapic acid-GO adduct, sinapic acid mono- and di-MGO adducts and 2,3-butanedione

463 adduct. Along with the theoretical exact masses and molecular formulas of the precursor ions,

464 we tentatively identified typical patterns of hydroxylalkylation reaction. Figure 5B

465 summarizes the fragmentation spectra of GO-sinapic acid adduct suggesting the loss of water

466 molecule [M-18]$^-$ at *m/z* 263.0564 and the consecutive losses of glyoxal, hydroxyl group and

467 the two -OCH$_3$ ether groups pointing at *m/z* 145.9355. In Figure 5C strong evidence suggests

468 for a double loss of $CO_2$ [M-44]$^-$ as revealed by the two signals at *m/z* 251.0569 and

469 207.0650. Furthermore, we hypothesized the removal of MGO, $C_3H_5O_2^{\cdot}$ [M-73.029] and the

470 loss of $C_3H_3O_2^{\cdot}$ [M-71.013] leading to the formation of the fragment at *m/z* 153.0556. For the

471  first time, we report the putative chemical structure of sinapic acid di-substituted with MGO

472  in Figure 5D. Again, the *m/z* 153.0556 suggested for the removal of both MGO moieties

473  ($C_3H_5O_2^•$) and $C_3H_3O_2^•$, while the peak at *m/z* 249.0403 can be resulting from the loss of

474  water from one of the secondary alcohols. Figure 5E outlines the putative chemical structure

475  of sinapic acid-2,3-butanedione adduct, its precursor ion at *m/z* 309.0985 and a product ion at

476  *m/z* 263.0552 indicated the loss of a HCOOH group [M-46]⁻. Overall, these putative adducts

477  corroborate prior findings of Navarro et al. (2018), which reported a direct MGO trapping of

478  50% in the presence of $0.095 \pm 0.001$ mg/mL of sinapic acid.

479  In Figure 6, we outlined the fragmentation spectra of caffeic acid (Figure 6A) and its adducts

480  (Figure 6 from B to D). In line to what observed for sinapic acid, caffeic acid shows a main

481  peak at *m/z* 135.0451 indicating the loss of $CO_2$ from the precursor ion [M-H]⁻ at *m/z*

482  179.0350, a typical mass spectrometry behaviour of hydroxycinnamic acid family. In line

483  with fragments in panel A, caffeic acid-GO adduct reveals a similar pattern with the loss GO

484  moiety, $C_2H_3O_2^•$ and the consequent formation of caffeic acid fragments combined with the

485  signal at *m/z* 135.0456 [M-$CO_2$-GO]⁻. This latter signal was reported also in Figure 5C

486  highlighting the interlinked loss of MGO and $CO_2$. Furthermore, we putatively identified

487  another loss of $CO_2$ peaking at *m/z* 207.0661in line to the fragmentation pattern of sinapic

488  acid-MGO adduct. Finally in Figure 6D, we report the chemical structure and the

489  fragmentation pattern of caffeic acid-2,3-butanedione adduct: in line with hydroxycinnamic

490  acid derivatives, we pinpointed the loss of $CO_2$, at *m/z* 221.0826. However, in this reaction

491  mixture, we did not notice any formation of caffeic acid-di-MGO adducts probably because

492  of the competitive role exerted by other polyphenols. Tandem MS spectra of caffeic acid and

493  caffeic acid-MGO adduct fully confirmed the results obtained in similar conditions (Zhang et

494  al., 2019).

495 **3.5. Assessment of the effect of HMW-BSGM, sinapic acid and caffeic acid on *in vitro***

496 **glycation of BSA by glucose**

497 To assess the mitigating effect of HMW-BSGM, sinapic acid and caffeic acid against the

498 formation of free fluorescent AGEs *in vitro*, the corresponding fluorescence intensities were

499 measured using AG as a positive control (final concentration in the reaction medium 0.57

500 mg/mL). Based on the findings of the time course study of DCs trapping, the final

501 concentrations in the incubation model system were 4, 0.14 and 0.11 mg/mL for HMW-

502 BSGM, sinapic and caffeic acids, respectively.

503 The mitigating effect of these compounds on free fluorescent AGEs occurrence in BSA-GLC

504 assay is shown in Figure 7. For the studied samples, considerable variations in the inhibitory

505 activity of AGEs formed ($p < 0.05$) were observed. AG showed the highest inhibitory

506 capacity (average inhibitory rate $93.8 \pm 0.6\%$) followed by HMW-BSGM ($79.3 \pm 3.8\%$). The

507 individual polyphenols exhibited the lowest reduction in the formation of fluorescent AGE,

508 with values of $53.4 \pm 1.5$ and $45.4 \pm 1.6\%$ for sinapic acid and caffeic acid, respectively. In

509 terms of AGEs mitigation, HMW-BSGM overperformed several natural seed products that

510 were comparatively tested at a concentration of 3.6 mg/mL, namely apricot (23.2%), peach

511 (20.7%), sesame (66.1%), almond and pomegranate seeds (61.7%). Only green pepper seeds

512 extract surpassed HMW-BSGM, inhibiting 91.9% of fluorescent AGEs in BSA-GLC model

513 system (Mesías et al., 2013).

514 **4. Conclusion**

515 The role of melanoidins during GI digestion represents a challenging, but intriguing topic.

516 The kind of chemical moieties occurring on these brown polymers and the corresponding

517 ability to block highly reactive compounds needs to be combined with the complexity of food

518 digesta and the enzymatic processes ongoing in the oxidizing environment occurring in the

519    GI tract. In a simplified model system consisting of incubation at 37 °C up to 168 h, we

520    demonstrated that, in line with other vegetable melanoidins as coffee and cocoa melanoidins,

521    HMW-BSGM is a valuable source of bioactive molecules. We envisaged that the local

522    accumulation of polyphenols in association with the melanoidin skeleton can work as a

523    sponge not only for transition metals, but also for α-dicarbonyls, thus limiting undesired

524    effects and reactions leading to potentially toxic molecules. Hydroxycinnamic derivatives

525    such as caffeic acid and its derivatives played a key role; their chemical nature was readily

526    prone to the reaction with α-dicarbonyls and, according to dedicated MS/MS and UV

527    experiments, we obtained that MGO is the preferred target, but similar reaction pathways can

528    be outlined for GO and 2,3-butanedione. Surprisingly, a similar behaviour was observed for

529    sinapic acid, suggesting that the multitude of possible combinations in nature can be further

530    enhanced by controlled thermal treatment able to expose bioactive moiety and improve the

531    functionality of foods ingredients.

544

545 **References**

546 Ahmad, S., Uddin, M., Shahab, U., Habib, S., Salman Khan, M., Alam, K., & Ali, A. (2014).

547     Glycoxidative damage to human DNA: Neo-antigenic epitopes on DNA molecule could be a

548     possible reason for autoimmune response in type 1 diabetes. *Glycobiology*, *24*(3), 281–291.

549     https://doi.org/10.1093/glycob/cwt109

550 Athanasios, M., Georgios, L., & Michael, K. (2007). A rapid microwave-assisted derivatization

551     process for the determination of phenolic acids in brewer's spent grains. *Food Chemistry*,

552     *102*(3), 606–611. https://doi.org/10.1016/j.foodchem.2006.05.040

553 Baynes, J. W., & Thorpe, S. R. (2000). Glycoxidation and lipoxidation in atherogenesis. *Free Radical*

554     *Biology and Medicine*, *28*(12), 1708–1716. https://doi.org/10.1016/S0891-5849(00)00228-8

555 Brings, S., Fleming, T., Freichel, M., Muckenthaler, M., Herzig, S., & Nawroth, P. (2017).

556     Dicarbonyls and advanced glycation end-products in the development of diabetic

557     complications and targets for intervention. *International Journal of Molecular Sciences*,

558     *18*(5), 984. https://doi.org/10.3390/ijms18050984

559 Chen, X.-Y., Huang, I.-M., Hwang, L. S., Ho, C.-T., Li, S., & Lo, C.-Y. (2014). Anthocyanins in

560     blackcurrant effectively prevent the formation of advanced glycation end products by trapping

561     methylglyoxal. *Journal of Functional Foods*, *8*, 259–268.

562     https://doi.org/10.1016/j.jff.2014.03.025

563 Coelho, C., Ribeiro, M., Cruz, A. C. S., Domingues, M. R. M., Coimbra, M. A., Bunzel, M., &

564     Nunes, F. M. (2014). Nature of phenolic compounds in coffee melanoidins. *Journal of*

565     *Agricultural and Food Chemistry*, *62*(31), 7843–7853. https://doi.org/10.1021/jf501510d

566 Davies, M. J. (2016). Protein oxidation and peroxidation. *Biochemical Journal*, *473*(7), 805–825.

567     https://doi.org/10.1042/BJ20151227

568 Delgado-Andrade, C., & Fogliano, V. (2018). Dietary advanced glycosylation end-products (dAGEs)

569     and melanoidins formed through the Maillard reaction: Physiological consequences of their

570     intake. *Annual Review of Food Science and Technology*, *9*, 271–291.

571     https://doi.org/10.1146/annurev-food-030117-012441

572     Deshpande, S. N., & Aguilar, A. A. (1975). Effects of roasting temperatures and gamma irradiation on

573           the content of chlorogenic acid, caffeic acid and soluble carbohydrates of coffee. *The*

574           *International Journal of Applied Radiation and Isotopes*, *26*(11), 656–661.

575           https://doi.org/10.1016/0020-708X(75)90021-6

576     Fogliano, V., & Morales, F. J. (2011). Estimation of dietary intake of melanoidins from coffee and

577           bread. *Food & Function*, *2*(2), 117–123. https://doi.org/10.1039/c0fo00156b

578     Gaens, K. H. J., Stehouwer, C. D. A., & Schalkwijk, C. G. (2013). Advanced glycation endproducts

579           and its receptor for advanced glycation endproducts in obesity. *Current Opinion in*

580           *Lipidology*, *24*(1), 4–11. https://doi.org/10.1097/MOL.0b013e32835aea13

581     Hellwig, M., Gensberger-Reigl, S., Henle, T., & Pischetsrieder, M. (2018). Food-derived 1,2-

582           dicarbonyl compounds and their role in diseases. *Seminars in Cancer Biology*, *49*, 1–8.

583           https://doi.org/10.1016/j.semcancer.2017.11.014

584     Hellwig, M., Humpf, H.-U., Hengstler, J., Mally, A., Vieths, S., & Henle, T. (2019). Quality criteria

585           for studies on dietary glycation compounds and human health: Opinion of the senate

586           commission on food safety (SKLM) of the German research foundation (DFG). *Journal of*

587           *Agricultural and Food Chemistry*, *67*(41), 11307–11311.

588           https://doi.org/10.1021/acs.jafc.9b04172

589     Hernanz, D., Nuñez, V., Sancho, A. I., Faulds, C. B., Williamson, G., Bartolomé, B., & Gómez-

590           Cordovés, C. (2001). Hydroxycinnamic scids and ferulic scid Dehydrodimers in barley and

591           processed barley. *Journal of Agricultural and Food Chemistry*, *49*(10), 4884–4888.

592           https://doi.org/10.1021/jf010530u

593     Herraiz, T., Peña, A., Mateo, H., Herraiz, M., & Salgado, A. (2022). Formation, characterization, and

594           occurrence of β-carboline alkaloids derived from α-dicarbonyl compounds and L -tryptophan.

595           *Journal of Agricultural and Food Chemistry*, *70*(29), 9143–9153.

596           https://doi.org/10.1021/acs.jafc.2c03187

597     Huang, Q., Wang, P., Zhu, Y., Lv, L., & Sang, S. (2017). Additive capacity of [6]-shogaol and

598           epicatechin to trap methylglyoxal. *Journal of Agricultural and Food Chemistry*, *65*(38),

599           8356–8362. https://doi.org/10.1021/acs.jafc.7b02917

600  Iglesias-Carres, L., Mas-Capdevila, A., Bravo, F. I., Aragonès, G., Muguerza, B., & Arola-Arnal, A.

601      (2019). Optimization of a polyphenol extraction method for sweet orange pulp (Citrus

602      sinensis L.) to identify phenolic compounds consumed from sweet oranges. *PLOS ONE*,

603      *14*(1), e0211267. https://doi.org/10.1371/journal.pone.0211267

604  Kahyaoglu, T., & Kaya, S. (2006). Modeling of moisture, color and texture changes in sesame seeds

605      during the conventional roasting. *Journal of Food Engineering*, *75*(2), 167–177.

606      https://doi.org/10.1016/j.jfoodeng.2005.04.011

607  Kasperovich, V. L., Grechushkin, A. I., Kupriyanov, A. V., & Miroshnikov, S. A. (2009). Technology

608      of utilizing brewery waste and use of the product obtained for feeding young bulls. *Russian*

609      *Agricultural Sciences*, *35*(4), 262–265. https://doi.org/10.3103/S1068367409040144

610  Lan, M., Li, H., Tao, G., Lin, J., Lu, M., Yan, R., & Huang, J. (2020). Effects of four bamboo derived

611      flavonoids on advanced glycation end products formation in vitro. *Journal of Functional*

612      *Foods*, *71*, 103976. https://doi.org/10.1016/j.jff.2020.103976

613  Ledbetter, M., Blidi, S., Ackon, S., Bruno, F., Sturrock, K., Pellegrini, N., & Fiore, A. (2021). Effect

614      of novel sequential soaking treatments on Maillard reaction products in potato and alternative

615      vegetable crisps. *Heliyon*, *7*(7), e07441. https://doi.org/10.1016/j.heliyon.2021.e07441

616  Lv, L., Shao, X., Wang, L., Huang, D., Ho, C.-T., & Sang, S. (2010). Stilbene glucoside from

617      polygonum multiflorum Thunb.: A novel natural inhibitor of advanced glycation end product

618      formation by trapping of methylglyoxal. *Journal of Agricultural and Food Chemistry*, *58*(4),

619      2239–2245. https://doi.org/10.1021/jf904122q

620  Maasen, K., Eussen, S. J. P. M., Scheijen, J. L. J. M., van der Kallen, C. J. H., Dagnelie, P. C.,

621      Opperhuizen, A., Stehouwer, C. D. A., van Greevenbroek, M. M. J., & Schalkwijk, C. G.

622      (2022). Higher habitual intake of dietary dicarbonyls is associated with higher corresponding

623      plasma dicarbonyl concentrations and skin autofluorescence: The Maastricht study. *The*

624      *American Journal of Clinical Nutrition*, *115*(1), 34–44. https://doi.org/10.1093/ajcn/nqab329

625  MassBank consortium and its contributors. (2020). *MassBank/MassBank-data: Release version*

626      *2020.06* (2020.06). Zenodo. https://doi.org/10.5281/ZENODO.3903207

627     McCarthy, A. L., O'Callaghan, Y. C., Neugart, S., Piggott, C. O., Connolly, A., Jansen, M. A. K.,

628          Krumbein, A., Schreiner, M., FitzGerald, R. J., & O'Brien, N. M. (2013). The

629          hydroxycinnamic acid content of barley and brewers' spent grain (BSG) and the potential to

630          incorporate phenolic extracts of BSG as antioxidants into fruit beverages. *Food Chemistry*,

631          *141*(3), 2567–2574. https://doi.org/10.1016/j.foodchem.2013.05.048

632     Meade, S. J., Miller, A. G., & Gerrard, J. A. (2003). The role of dicarbonyl compounds in non-

633          enzymatic crosslinking: A structure–activity study. *Bioorganic & Medicinal Chemistry*,

634          *11*(6), 853–862. https://doi.org/10.1016/S0968-0896(02)00564-3

635     Mesías, M., & Delgado-Andrade, C. (2017). Melanoidins as a potential functional food ingredient.

636          *Current Opinion in Food Science*, *14*, 37–42. https://doi.org/10.1016/j.cofs.2017.01.007

637     Mesías, M., Navarro, M., Gökmen, V., & Morales, F. J. (2013). Antiglycative effect of fruit and

638          vegetable seed extracts: Inhibition of AGE formation and carbonyl-trapping abilities. *Journal*

639          *of the Science of Food and Agriculture*, *93*(8), 2037–2044. https://doi.org/10.1002/jsfa.6012

640     Monente, C., Ludwig, I. A., Irigoyen, A., De Peña, M.-P., & Cid, C. (2015). Assessment of total (free

641          and bound) phenolic compounds in spent coffee extracts. *Journal of Agricultural and Food*

642          *Chemistry*, *63*(17), 4327–4334. https://doi.org/10.1021/acs.jafc.5b01619

643     Morales, F. J., Somoza, V., & Fogliano, V. (2012). Physiological relevance of dietary melanoidins.

644          *Amino Acids*, *42*(4), 1097–1109. https://doi.org/10.1007/s00726-010-0774-1

645     Moreira, A. S. P., Nunes, F. M., Domingues, M. R., & Coimbra, M. A. (2012). Coffee melanoidins:

646          Structures, mechanisms of formation and potential health impacts. *Food & Function*, *3*(9),

647          903. https://doi.org/10.1039/c2fo30048f

648     Moreira, A. S. P., Nunes, F. M., Simões, C., Maciel, E., Domingues, P., Domingues, M. R. M., &

649          Coimbra, M. A. (2017). Transglycosylation reactions, a main mechanism of phenolics

650          incorporation in coffee melanoidins: Inhibition by Maillard reaction. *Food Chemistry*, *227*,

651          422–431. https://doi.org/10.1016/j.foodchem.2017.01.107

652     Navarro, M., de Falco, B., Morales, F. J., Daliani, D., & Fiore, A. (2018). Explorative investigation of

653          the anti-glycative effect of a rapeseed by-product extract. *Food & Function*, *9*(11), 5674–

654          5681. https://doi.org/10.1039/C8FO01408F

655    Nigam, P. S. (2017). An overview: Recycling of solid barley waste generated as a by-product in

656        distillery and brewery. *Waste Management*, *62*, 255–261.

657        https://doi.org/10.1016/j.wasman.2017.02.018

658    Oracz, J., Nebesny, E., & Żyżelewicz, D. (2019). Identification and quantification of free and bound

659        phenolic compounds contained in the high-molecular weight melanoidin fractions derived

660        from two different types of cocoa beans by UHPLC-DAD-ESI-HR-MSn. *Food Research*

661        *International*, *115*, 135–149. https://doi.org/10.1016/j.foodres.2018.08.028

662    Palma-Duran, S. A., Lean, M. E. J., & Combet, E. (2016). Roasted instant coffees: Analysis of

663        (poly)phenols and melanoidins antioxidant capacity, potassium and sodium contents.

664        *Proceedings of the Nutrition Society*, *75*(OCE2), E63.

665        https://doi.org/10.1017/S0029665116000537

666    Peng, X., Cheng, K.-W., Ma, J., Chen, B., Ho, C.-T., Lo, C., Chen, F., & Wang, M. (2008). Cinnamon

667        bark proanthocyanidins as reactive carbonyl scavengers to prevent the formation of advanced

668        glycation endproducts. *Journal of Agricultural and Food Chemistry*, *56*(6), 1907–1911.

669        https://doi.org/10.1021/jf073065v

670    Quifer-Rada, P., Vallverdú-Queralt, A., Martínez-Huélamo, M., Chiva-Blanch, G., Jáuregui, O.,

671        Estruch, R., & Lamuela-Raventós, R. (2015). A comprehensive characterisation of beer

672        polyphenols by high resolution mass spectrometry (LC–ESI-LTQ-Orbitrap-MS). *Food*

673        *Chemistry*, *169*, 336–343. https://doi.org/10.1016/j.foodchem.2014.07.154

674    Rabbani, N., & Thornalley, P. J. (2012). Methylglyoxal, glyoxalase 1 and the dicarbonyl proteome.

675        *Amino Acids*, *42*(4), 1133–1142. https://doi.org/10.1007/s00726-010-0783-0

676    Re, R., Pellegrini, N., Proteggente, A., Pannala, A., Yang, M., & Rice-Evans, C. (1999). Antioxidant

677        activity applying an improved ABTS radical cation decolorization assay. *Free Radical*

678        *Biology and Medicine*, *26*(9–10), 1231–1237. https://doi.org/10.1016/S0891-5849(98)00315-

679        3

680    Robertson, J. A., I'Anson, K. J. A., Treimo, J., Faulds, C. B., Brocklehurst, T. F., Eijsink, V. G. H., &

681        Waldron, K. W. (2010). Profiling brewers' spent grain for composition and microbial ecology

682          at the site of production. *LWT - Food Science and Technology*, *43*(6), 890–896.

683          https://doi.org/10.1016/j.lwt.2010.01.019

684 Rogalla, P., Lembcke, A., Rückert, J. C., Hein, E., Bollow, M., Rogalla, N. E., & Hamm, B. (2005).

685          Spasmolysis at CT colonography: Butyl scopolamine versus glucagon. *Radiology*, *236*(1),

686          184–188. https://doi.org/10.1148/radiol.2353040007

687 Sato, T., Iwaki, M., Shimogaito, N., Wu, X., Yamagishi, S., & Takeuchi, M. (2006). TAGE (Toxic

688          AGEs) theory in diabetic complications. *Current Molecular Medicine*, *6*(3), 351–358.

689          https://doi.org/10.2174/156652406776894536

690 Schulz, M., Borges, G. da S. C., Gonzaga, L. V., Seraglio, S. K. T., Olivo, I. S., Azevedo, M. S.,

691          Nehring, P., de Gois, J. S., de Almeida, T. S., Vitali, L., Spudeit, D. A., Micke, G. A., Borges,

692          D. L. G., & Fett, R. (2015). Chemical composition, bioactive compounds and antioxidant

693          capacity of juçara fruit (Euterpe edulis Martius) during ripening. *Food Research*

694          *International*, *77*, 125–131. https://doi.org/10.1016/j.foodres.2015.08.006

695 Sergi, D., Boulestin, H., Campbell, F. M., & Williams, L. M. (2021). The role of dietary advanced

696          glycation end products in metabolic dysfunction. *Molecular Nutrition & Food Research*,

697          *65*(1), 1900934. https://doi.org/10.1002/mnfr.201900934

698 Singleton, V. L., Orthofer, R., & Lamuela-Raventós, R. M. (1999). Analysis of total phenols and

699          other oxidation substrates and antioxidants by means of folin-ciocalteu reagent. In L. Packer

700          (Ed.), *Methods in Enzymology* (pp. 152–178). Elsevier. https://doi.org/10.1016/S0076-

701          6879(99)99017-1

702 Snelson, M., Tan, S. M., Clarke, R. E., de Pasquale, C., Thallas-Bonke, V., Nguyen, T.-V., Penfold, S.

703          A., Harcourt, B. E., Sourris, K. C., Lindblom, R. S., Ziemann, M., Steer, D., El-Osta, A.,

704          Davies, M. J., Donnellan, L., Deo, P., Kellow, N. J., Cooper, M. E., Woodruff, T. M., …

705          Coughlan, M. T. (2021). Processed foods drive intestinal barrier permeability and

706          microvascular diseases. *Science Advances*, *7*(14), eabe4841.

707          https://doi.org/10.1126/sciadv.abe4841

708  Summa, C., Raposo, F. C., McCourt, J., Scalzo, R. L., Wagner, K.-H., Elmadfa, I., & Anklam, E.

709      (2006). Effect of roasting on the radical scavenging activity of cocoa beans. *European Food*

710      *Research and Technology*, *222*(3–4), 368–375. https://doi.org/10.1007/s00217-005-0005-2

711  Szwajgier, D., Waśko, A., Targoński, Z., Niedźwiadek, M., & Bancarzewska, M. (2010). The use of a

712      novel ferulic acid esterase from Lactobacillus acidophilus K1 for the release of phenolic acids

713      from brewer's spent grain. *Journal of the Institute of Brewing*, *116*(3), 293–303.

714      https://doi.org/10.1002/j.2050-0416.2010.tb00434.x

715  Totlani, V. M., & Peterson, D. G. (2006). Epicatechin carbonyl-trapping reactions in aqueous

716      Maillard systems: Identification and structural elucidation. *Journal of Agricultural and Food*

717      *Chemistry*, *54*(19), 7311–7318. https://doi.org/10.1021/jf061244r

718  Troise, A. D., Fiore, A., Colantuono, A., Kokkinidou, S., Peterson, D. G., & Fogliano, V. (2014).

719      Effect of Olive Mill Wastewater Phenol Compounds on Reactive Carbonyl Species and

720      Maillard Reaction End-Products in Ultrahigh-Temperature-Treated Milk. *Journal of*

721      *Agricultural and Food Chemistry*, *62*(41), Article 41. https://doi.org/10.1021/jf503329d

722  Van den Eynde, M. D. G., Geleijnse, J. M., Scheijen, J. L. J. M., Hanssen, N. M. J., Dower, J. I.,

723      Afman, L. A., Stehouwer, C. D. A., Hollman, P. C. H., & Schalkwijk, C. G. (2018).

724      Quercetin, but not epicatechin, decreases plasma concentrations of methylglyoxal in adults in

725      a randomized, double-blind, placebo-controlled, crossover trial with pure flavonoids. *The*

726      *Journal of Nutrition*, *148*(12), 1911–1916. https://doi.org/10.1093/jn/nxy236

727  Vitaglione, P., Fogliano, V., & Pellegrini, N. (2012). Coffee, colon function and colorectal cancer.

728      *Food & Function*, *3*(9), 916. https://doi.org/10.1039/c2fo30037k

729  Voziyan, P. A., Metz, T. O., Baynes, J. W., & Hudson, B. G. (2002). A post-amadori inhibitor

730      pyridoxamine also inhibits chemical modification of proteins by scavenging carbonyl

731      intermediates of carbohydrate and lipid degradation. *Journal of Biological Chemistry*, *277*(5),

732      3397–3403. https://doi.org/10.1074/jbc.M109935200

733  Wu, J.-W., Hsieh, C.-L., Wang, H.-Y., & Chen, H.-Y. (2009). Inhibitory effects of guava (Psidium

734      guajava L.) leaf extracts and its active compounds on the glycation process of protein. *Food*

735      *Chemistry*, *113*(1), 78–84. https://doi.org/10.1016/j.foodchem.2008.07.025

736    Youn, K.-S., & Chung, H.-S. (2012). Optimization of the roasting temperature and time for

737        preparation of coffee-like maize beverage using the response surface methodology. *LWT -*

738        *Food Science and Technology*, *46*(1), 305–310. https://doi.org/10.1016/j.lwt.2011.09.014

739    Zhang, H., Zhang, H., Troise, A. D., & Fogliano, V. (2019). Melanoidins from coffee, cocoa, and

740        bread are able to scavenge α-dicarbonyl compounds under simulated physiological

741        conditions. *Journal of Agricultural and Food Chemistry*, *67*(39), 10921–10929.

742        https://doi.org/10.1021/acs.jafc.9b03744

743    Zhang, S., Xiao, L., Lv, L., & Sang, S. (2020). Trapping methylglyoxal by myricetin and Its

744        metabolites in mice. *Journal of Agricultural and Food Chemistry*, *68*(35), 9408–9414.

745        https://doi.org/10.1021/acs.jafc.0c03471

746
747

748 Table 1. Content of released phenolic compounds (mg/100 g dry weight) from high molecular
749 weight brewer's spent grain melanoidins after acidic and alkaline treatments. All values are
750 expressed as mean ± SD ($n$ = 3). n.d., not detected.

| | Acidic hydrolysis | Alkaline hydrolysis |
|---|---|---|
| **Phenolic acids** | | |
| *Hydroxycinnamic acids* | | |
| Ferulic acid | 54.68 ± 5.34 aA | 26.99 ± 3.51 aB |
| p-Coumaric acid | 7.55 ± 0.60 bA | 5.67 ± 0.31 bB |
| Sinapic acid | 7.55 ± 1.31 bA | 4.12 ± 0.94 bB |
| Caffeic acid | 7.66 ± 0.56 bA | 5.39 ± 0.30 bB |
| **Total*** | **77.44 ± 2.47 aA** | **42.17 ± 1.76 aB** |
| *Hydroxybenzoic acids* | | |
| Syringic acid | 5.39 ± 0.30 aA | 4.38 ± 0.23 aB |
| 4-Hydroxybenzoic acid | 3.54 ± 0.15 bA | 2.09 ± 0.22 bB |
| Benzoic acid | 2.68 ± 0.26 cA | 2.40 ± 0.20 bA |
| Protocatechuic acid | 0.93 ± 0.02 dA | 0.54 ± 0.05 cB |
| Gallic acid | 0.44 ± 0.02 eA | 0.41 ± 0.08 cA |
| Vanillic acid | n.d. fA | 2.90 ± 0.13 bB |
| **Total*** | **12.98 ± 0.63 bA** | **12.72 ± 0.39 bA** |
| **Flavonoids** | | |
| *Flavanols* | | |
| (+)-Catechin | 2.75 ± 0.08 A | 1.72 ± 0.32 B |
| **Other polyphenols** | | |
| *Hydroxybenzaldehydes* | | |
| Vanillin | 0.27 ± 0.05 A | 1.22 ± 0.24 B |

751 Different uppercase letters in the same row indicate significant differences (p < 0.05) according to
752 Student's' t test. Different lowercase letters in the same column within the same phenolic sub-group
753 indicate significant differences ($p$ < 0.05) according to Tukey's HSD test. *Total hydroxycinnamic
754 acids and total hydroxybenzoic acids were statistically compared separately using the student's' t test.
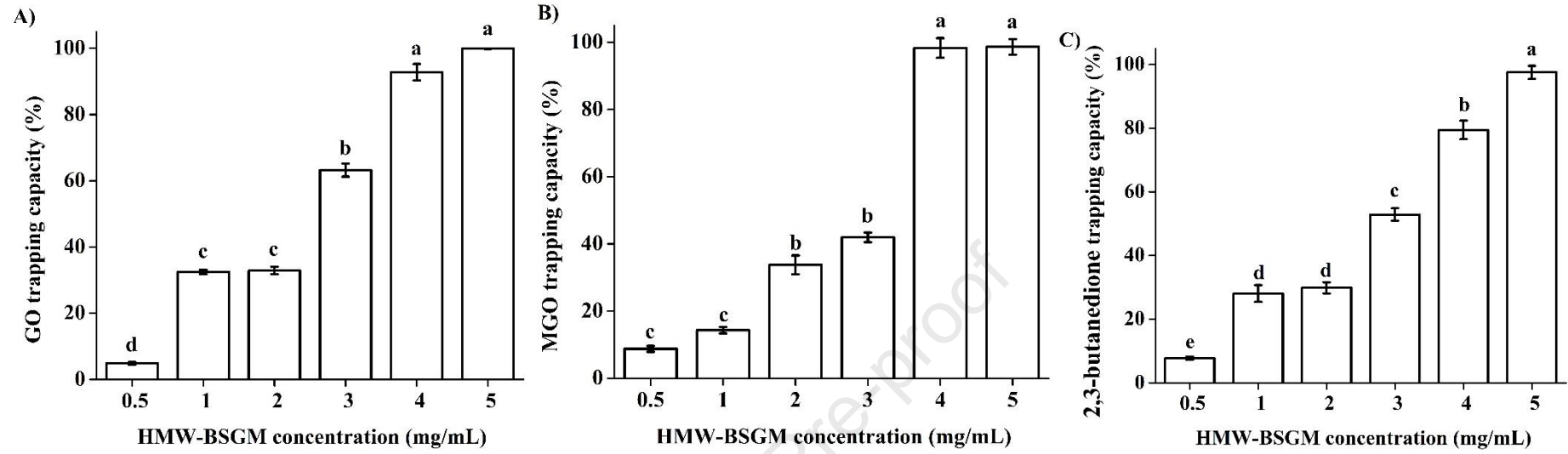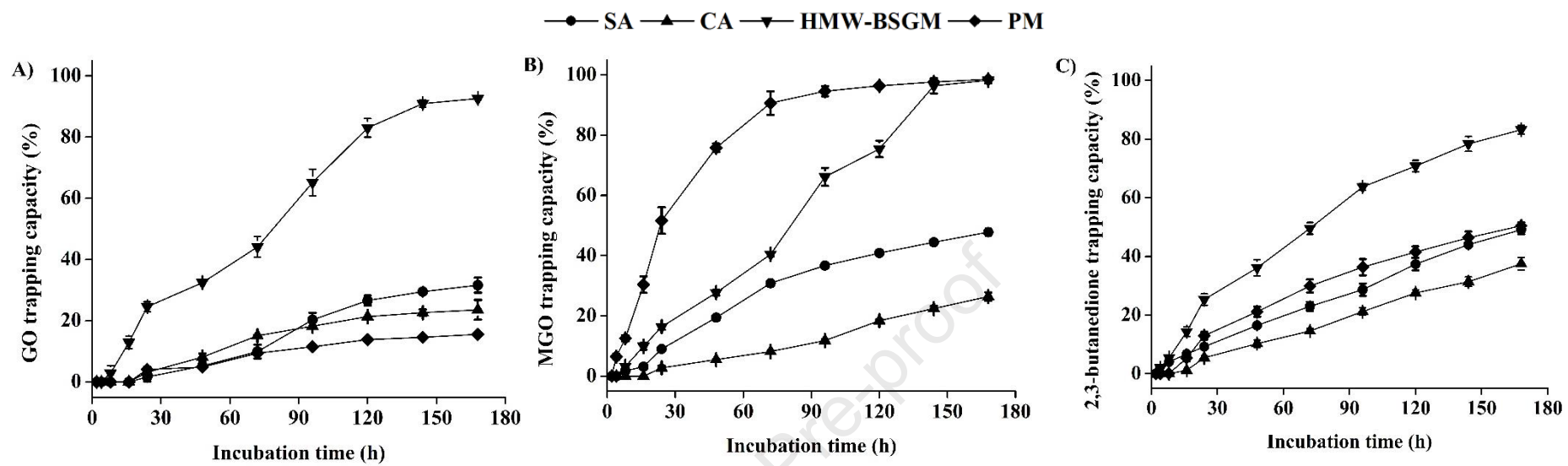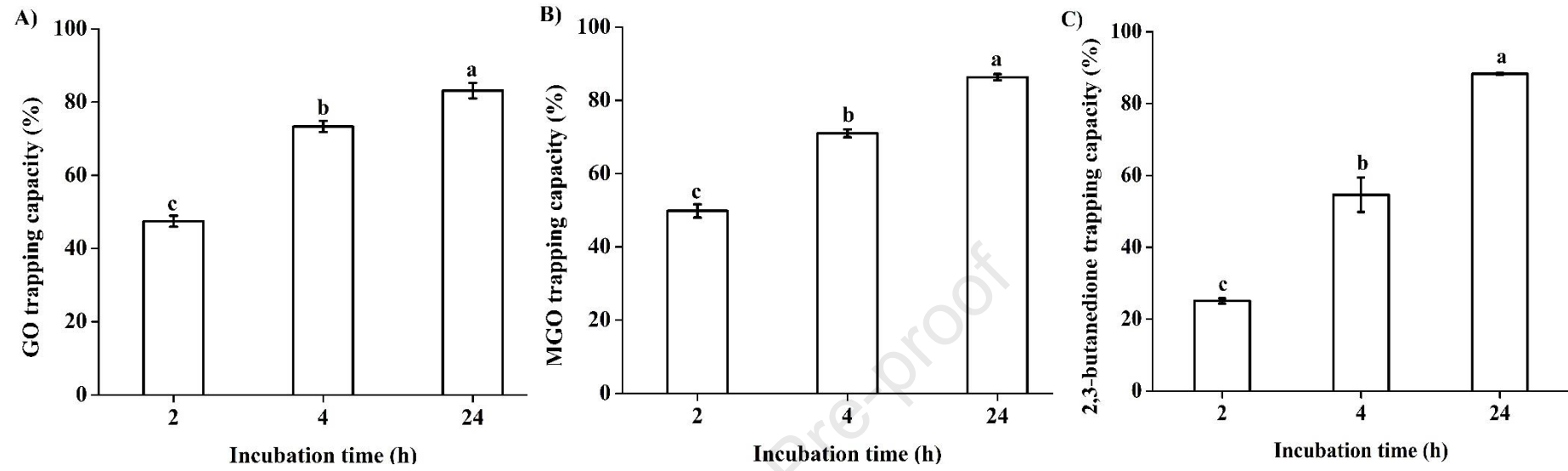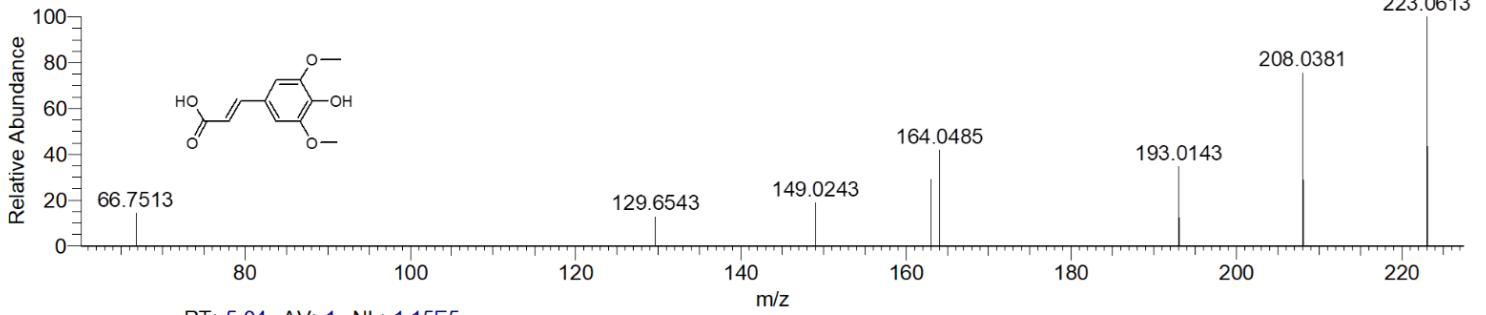
755

Table 1. Content of released phenolic compounds (mg/100 g dry weight) from high-molecular-weight brewer's spent grain melanoidins after acidic and alkaline treatments. All values are expressed as mean ± SD ($n$ = 3). n.d., not detected.

| | Acidic hydrolysis | Alkaline hydrolysis |
|---|---|---|
| **Phenolic acids** | | |
| | | |
| *Hydroxycinnamic acids* | | |
| Ferulic acid | 54.68 ± 5.34 aA | 26.99 ± 3.51 aB |
| p-Coumaric acid | 7.55 ± 0.60 bA | 5.67 ± 0.31 bB |
| Sinapic acid | 7.55 ± 1.31 bA | 4.12 ± 0.94 bB |
| Caffeic acid | 7.66 ± 0.56 bA | 5.39 ± 0.30 bB |
| **Total\*** | **77.44 ± 2.47 aA** | **42.17 ± 1.76 aB** |
| | | |
| *Hydroxybenzoic acids* | | |
| Syringic acid | 5.39 ± 0.30 aA | 4.38 ± 0.23 aB |
| 4-Hydroxybenzoic acid | 3.54± 0.15 bA | 2.09 ± 0.22 bB |
| Benzoic acid | 2.68 ± 0.26 cA | 2.40 ± 0.20 bA |
| Protocatechuic acid | 0.93 ± 0.02 dA | 0.54 ± 0.05 cB |
| Gallic acid | 0.44 ± 0.02 eA | 0.41 ± 0.08 cA |
| Vanillic acid | n.d. fA | 2.90 ± 0.13 bB |
| **Total\*** | **12.98 ± 0.63 bA** | **12.72 ± 0.39 bA** |
| | | |
| **Flavonoids** | | |
| | | |
| *Flavanols* | | |
| (+)-Catechin | 2.75 ± 0.08 A | 1.72 ± 0.32 B |
| | | |
| **Other polyphenols** | | |
| | | |
| *Hydroxybenzaldehydes* | | |
| Vanillin | 0.27 ± 0.05 A | 1.22 ± 0.24 B |

Different uppercase letters in the same row indicate significant differences (p < 0.05) according to Student's' t test. Different lowercase letters in the same column within the same phenolic sub-group indicate significant differences ($p$ < 0.05) according to Tukey's HSD test. *Total hydroxycinnamic acids and total hydroxybenzoic acids were statistically compared separately using the student's' t test.

A)

B)

C)

A) B) C) SA — CA — HMW-BSGM — PM

GO trapping capacity (%) vs Incubation time (h); MGO trapping capacity (%) vs Incubation time (h); 2,3-butanedione trapping capacity (%) vs Incubation time (h)

A) GO trapping capacity (%) vs Incubation time (h)

B) MGO trapping capacity (%) vs Incubation time (h)

C) 2,3-butanedione trapping capacity (%) vs Incubation time (h)
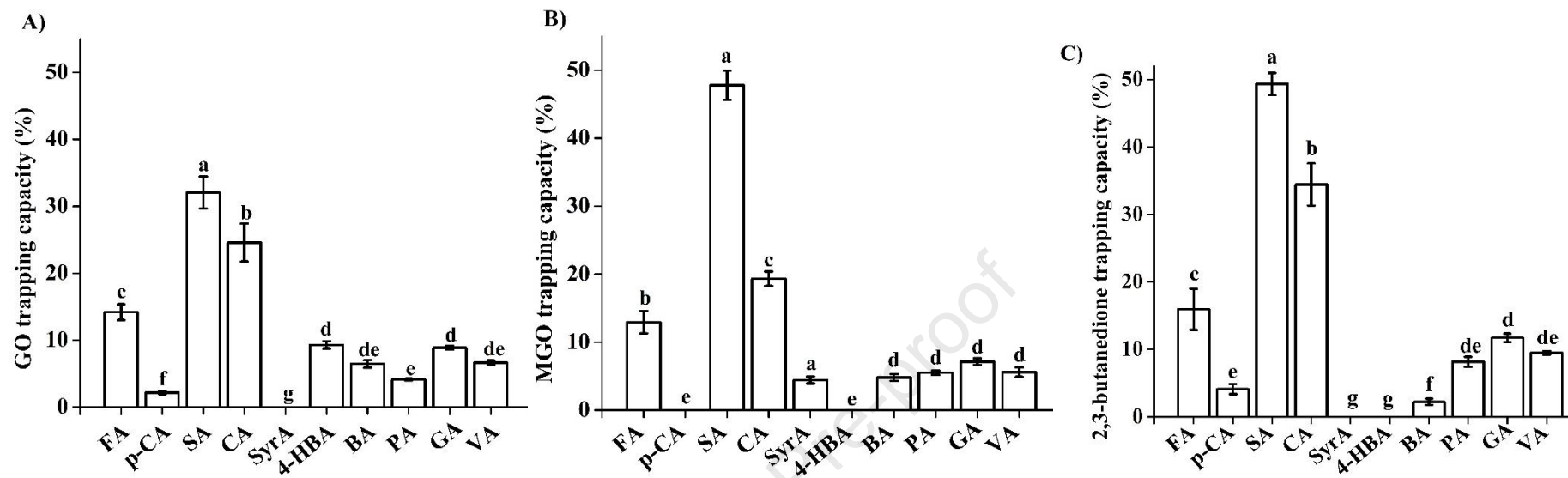
RT: 6.43 AV: 1 NL: 7.79E4
F: FTMS - p ESI Full ms2 223.0612@hcd30.00 [49.6065-248.0324]

**A**

RT: 5.04 AV: 1 NL: 1.15E5
F: FTMS - p ESI Full ms2 281.0667@hcd30.00 [50.0000-307.1980]

**B**
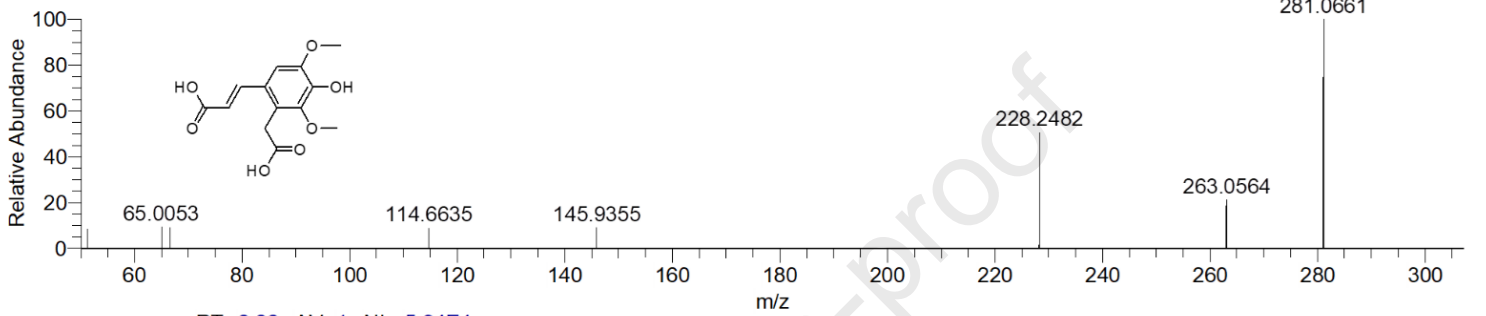
RT: 6.66 AV: 1 NL: 5.94E4
F: FTMS - p ESI Full ms2 295.0823@hcd30.00 [50.0000-321.4939]

**C**
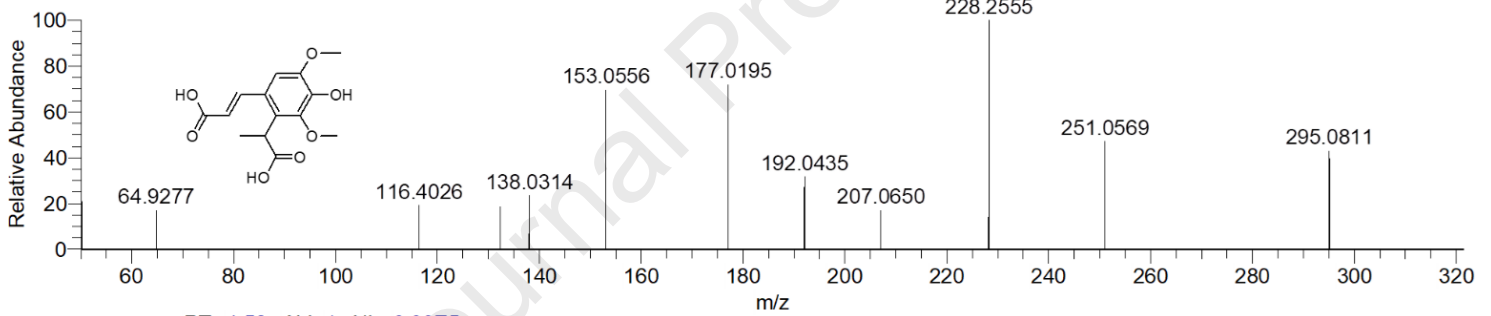
RT: 4.56 AV: 1 NL: 9.99E5
F: FTMS - p ESI Full ms2 367.1035@hcd30.00 [50.0000-394.9556]

**D**
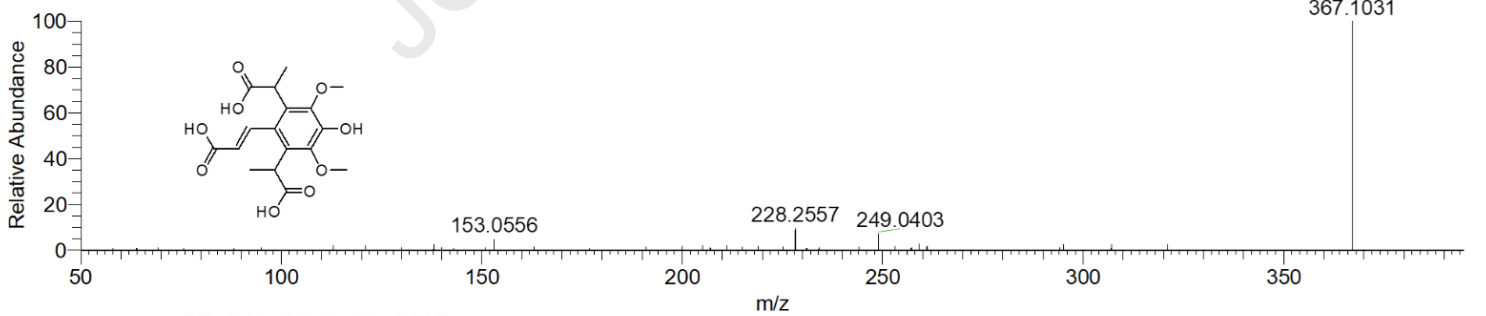
RT: 6.21 AV: 1 NL: 6.79E4
F: FTMS - p ESI Full ms2 309.0980@hcd30.00 [50.0000-335.7900]

**E**
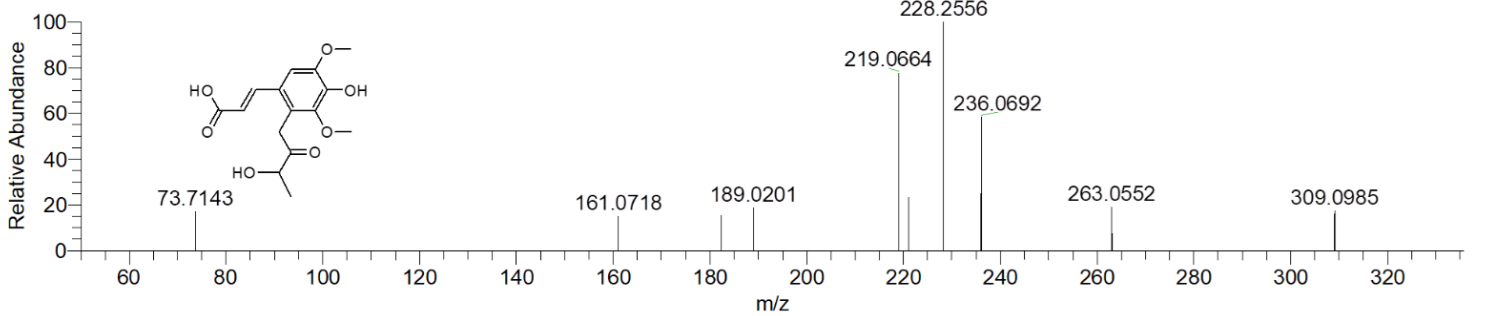
RT: 5.16 AV: 1 NL: 5.26E8
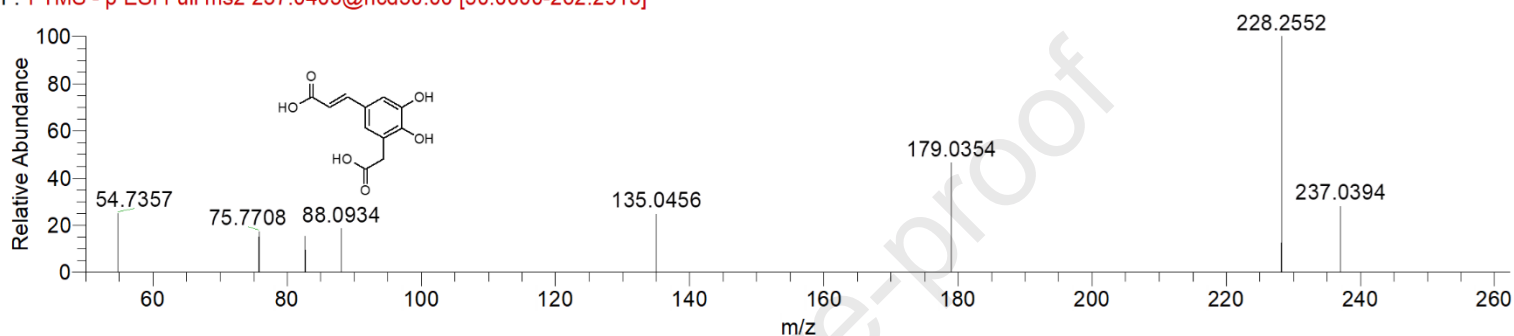F: FTMS - p ESI Full ms2 179.0350@hcd30.00 [40.6251-203.1257]

**A**
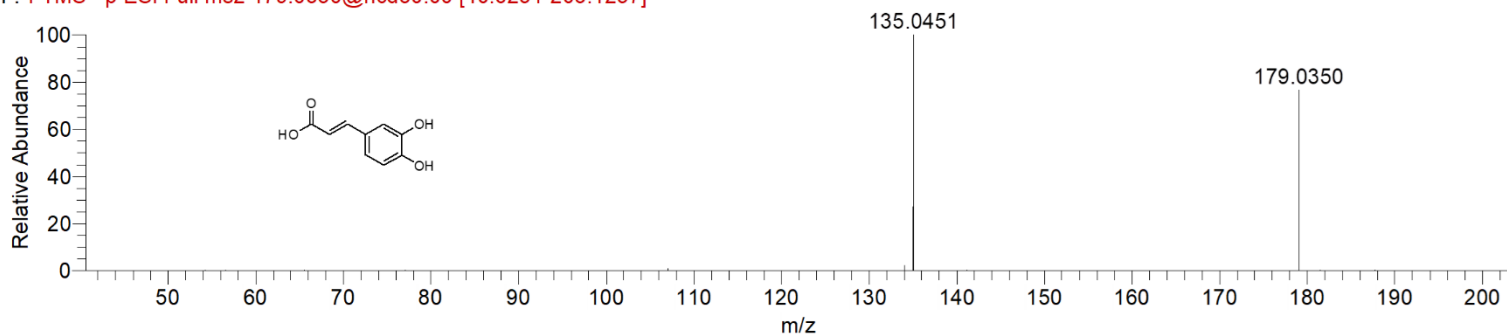
RT: 5.84 AV: 1 NL: 6.07E4
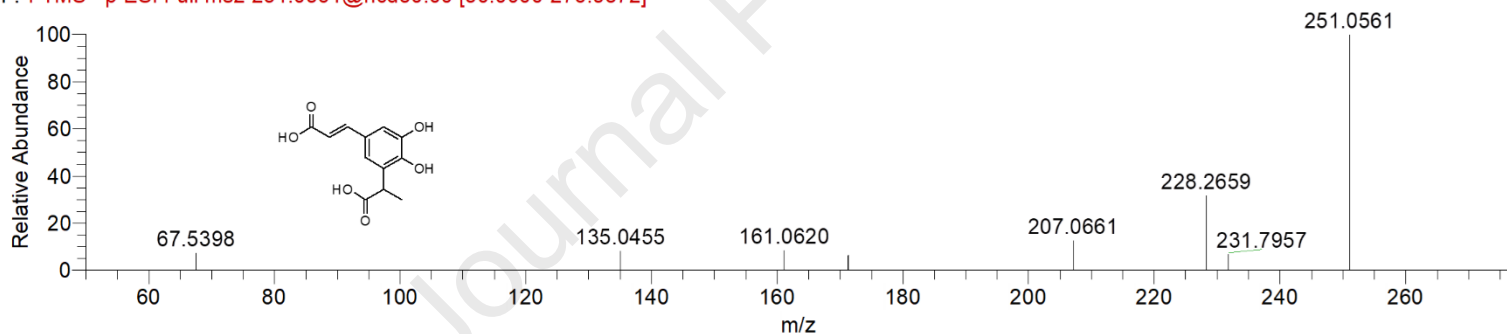F: FTMS - p ESI Full ms2 237.0405@hcd30.00 [50.0000-262.2913]

**B**

RT: 4.78 AV: 1 NL: 1.53E5
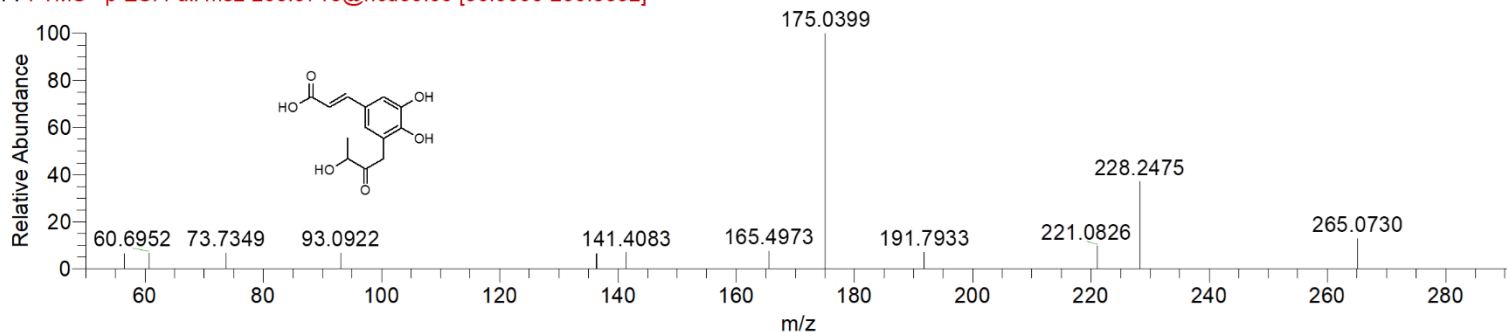F: FTMS - p ESI Full ms2 251.0561@hcd30.00 [50.0000-276.5872]

**C**

RT: 6.48 AV: 1 NL: 1.50E5
F: FTMS - p ESI Full ms2 265.0718@hcd30.00 [50.0000-290.8832]
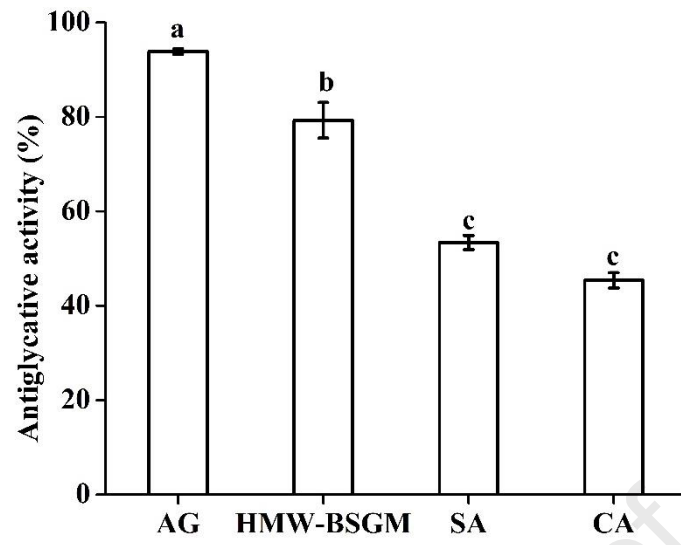
**D**

Figure 1. GO (A), MGO (B), and 2,3-butanedione (C) trapping capacities of the phenolic acids identified in high-molecular weight brewer's spent grain melanoidins at 168 h. FA (0.12 mg/mL), p-CA (0.11 mg/mL), SA (0.14 mg/mL), CA (0.11 mg/mL), SyrA (0.12 mg/mL), 4-HBA (0.09 mg/mL), BA (0.07 mg/mL), PA (0.09 mg/mL), GA (0.10 mg/mL) and VA (0.10 mg/mL). All concentration values correspond to 0.64 mmol/L. Results are expressed as mean ± SD for $n = 3$. Bars with different letters indicate significant differences according to Tukey's HSD test at $p < 0.05$. Glyoxal (GO); methylglyoxal (MGO); ferulic acid (FA); p-coumaric acid (p-CA); sinapic acid (SA); caffeic acid (CA); syringic acid (SyrA); 4-hydroxybenzoic acid (4-HBA); benzoic acid (BA); protocatechuic acid (PA); gallic acid (GA); vanillic acid (VA).

Figure 2. GO (A), MGO (B), and 2,3-butanedione (C) trapping capacities of high-molecular- weight brewer's spent grain melanoidins at different concentrations (0.5–5 mg/mL) at 168 h. Results are expressed as mean ± SD for $n = 3$. Bars with different letters indicate significant differences according to Tukey's HSD test at $p < 0.05$. Glyoxal (GO); methylglyoxal (MGO).

Figure 3. Time-course of GO (A), MGO (B), and 2,3-butanedione (C) trapping capacity of SA (0.14 mg/mL), CA (0.11 mg/mL), HMW-BSGM (4 mg/mL), and PM (0.11 mg/mL). Results are expressed as mean ± SD for $n = 3$. Glyoxal (GO); methylglyoxal (MGO); high-molecular-weight brewer's spent grain melanoidins (HMW-BSGM); sinapic acid (SA); caffeic acid (CA); pyridoxamine (PM).

Figure 4. Dicarbonyl trapping capacity of high-molecular weight brewer's spent grain melanoidins (5 mg/mL) within 24 h under simulated physiological conditions. The concentration of dicarbonyls and melanoidins was calculated according to the estimated daily intake. Results are expressed as mean ± SD for $n = 3$. Bars with different letters indicate significant differences according to Tukey's HSD test at $p < 0.05$. Glyoxal (GO); methylglyoxal (MGO).

Figure 5. Tandem mass spectra of sinapic acid (panel A) and sinapic acid-dicarbonyls adducts (panels B, C, D, E). Profile data were acquired in negative product ion scan mode, working in targeted MS$^2$ according to molecular formulas and $m/z$ extracted in full scan mode (see supplementary table 1). Normalized collision energy was set at 30% for all the scan experiments. Putative chemical formulas in each box were based on hypothesized fragmentation pathway and hydroxyalkylation reaction.

Figure 6. Tandem mass spectra of caffeic acid (panel A) and caffeic acid-dicarbonyls adducts (panels B, C, D). Profile data were acquired in negative product ion scan mode, working in targeted MS$^2$ according to molecular formulas and $m/z$ extracted in full scan mode (see supplementary table 1). Normalized collision energy was set at 30% for all the scan experiments. Putative chemical formulas in each box were based on hypothesized fragmentation pathway and hydroxyalkylation reaction.

Figure 7. Antiglycative activity of AG (0.57 mg/mL), HMW-BSGM (4 mg/mL), SA (0.14 mg/mL) and CA (0.11 mg/ mL) in BSA-GLC assay. Results are expressed as mean ± SD for $n = 3$. Bars with different letters indicate significant differences according to Tukey's HSD test at $p < 0.05$. Aminoguanidine (AG); high-molecular-weight brewer's spent grain melanoidins (HMW-BSGM); sinapic acid (SA); caffeic acid (CA).

**Highlights:**

A novel use of brewer's spent gain is discussed.

The polyphenolic profile of brewer's spent grain melanoidins is established.

Brewer's spent grain melanoidins trapped α-dicarbonyls in a simplified model system.

Brewer's spent grain melanoidins inhibited the formation of free fluorescent AGEs.

The putative adduct of sinapic acid-di-MGO is reported for the first time.

**Declaration of interests**

☒ The authors declare that they have no known competing financial interests or personal relationships that could have appeared to influence the work reported in this paper.

☐The authors declare the following financial interests/personal relationships which may be considered as potential competing interests: